

Transcriptional Maintenance of Pancreatic Acinar Identity, Differentiation, and Homeostasis by PTF1A

Chinh Q. Hoang,^a Michael A. Hale,^a Ana C. Azevedo-Pouly,^a Hans P. Elsässer,^b Tye G. Deering,^a Spencer G. Willet,^c Fong C. Pan,^c Mark A. Magnuson,^d Christopher V. E. Wright,^c Galvin H. Swift,^a Raymond J. MacDonald^a

Department of Molecular Biology, University of Texas Southwestern Medical Center, Dallas, Texas, USA^a; Department of Cytobiology, Philipps University of Marburg, Marburg, Germany^b; Program in Developmental Biology and Department of Cell and Developmental Biology, Vanderbilt University School of Medicine, Nashville, Tennessee, USA^c; Department of Molecular Physiology and Biophysics and Center for Stem Cell Biology, Vanderbilt University Medical Center, Nashville, Tennessee, USA^d

Maintenance of cell type identity is crucial for health, yet little is known of the regulation that sustains the long-term stability of differentiated phenotypes. To investigate the roles that key transcriptional regulators play in adult differentiated cells, we examined the effects of depletion of the developmental master regulator PTF1A on the specialized phenotype of the adult pancreatic acinar cell *in vivo*. Transcriptome sequencing and chromatin immunoprecipitation sequencing results showed that PTF1A maintains the expression of genes for all cellular processes dedicated to the production of the secretory digestive enzymes, a highly attuned surveillance of unfolded proteins, and a heightened unfolded protein response (UPR). Control by PTF1A is direct on target genes and indirect through a ten-member transcription factor network. Depletion of PTF1A causes an imbalance that overwhelms the UPR, induces cellular injury, and provokes acinar metaplasia. Compromised cellular identity occurs by derepression of characteristic stomach genes, some of which are also associated with pancreatic ductal cells. The loss of acinar cell homeostasis, differentiation, and identity is directly relevant to the pathologies of pancreatitis and pancreatic adenocarcinoma.

Loss of cellular identity has long been associated with tissue injury and a first step in cancer progression (for examples, see references 1 and 2). Maintenance of a specific cellular phenotype depends on the continued transcription of cell-type-specific genes, largely through open chromatin architecture (3, 4) maintained by a small group of lineage-restricted DNA-binding transcription factors (TFs) (5, 6) that establish a unique transcriptional regulatory network (7). Many physiologic or pathophysiologic perturbations can affect the differentiated state of a cell quantitatively, but fewer affect the state of differentiation qualitatively. Qualitative changes involve the acquisition of characteristics of another cell type (or types), often defined by one or a few cell-specific markers, in addition to the diminution of the original phenotype. Despite progress with cellular reprogramming (for example, see reference 8), the molecular and genetic mechanisms that maintain cellular identity within the context of adult organs remain incompletely understood. In this report, we show that inactivation of the transcriptional regulatory gene *Ptf1a* in adult pancreatic acinar cells has pleiotropic effects on gene expression that cause quantitative and multigene qualitative changes of acinar differentiation.

The acinar cell of the pancreas has been an informative model of terminal cellular differentiation (9). Common cellular processes are greatly exaggerated in support of the prodigious synthesis, processing, storage, and exocytosis of secretory proteins. The pancreatic acinar cell has the most ribosomes (10) and the highest rate of protein synthesis (11) of any mammalian somatic cell; it synthesizes, stores, and secretes its weight in protein daily. Specialized cellular functions and architecture establish the machinery for this extreme level of protein synthesis. Whereas the embryonic development of the pancreas, including the acinar compartment, is well studied, relatively little is known of the transcriptional mechanisms that maintain the extreme phenotype and cell type identity of the mature pancreatic acinar cell.

PTF1A, a sequence-specific, DNA-binding, basic helix-loop-helix (bHLH) TF, is among the best-studied regulators of pancre-

atic development. *Ptf1a*-null embryos fail pancreatic organogenesis at its earliest stage; only a tiny rudiment of pancreatic/hepatobiliary-like duct forms (12, 13). *Ptf1a* is required early for the expansion of the nascent pancreatic bud epithelium and its commitment to pancreatic fate (12), including the formation of pancreatic multipotent progenitor cells (14), and is believed to drive the subsequent specification and differentiation of the acinar lineage (15, 16). *Ptf1a* expression in adults is nearly exclusively restricted to acinar cells of the pancreas and drives transcription of several acinar cell markers (17–21); other exocrine glands do not use *Ptf1a*. PTF1A disappears during acinar-to-ductal metaplasia caused by acinar cell injury (22) and during the formation of acinus-derived precancerous lesions, known as PanINs (23). Conversely, inactivation of *Ptf1a* in adult acinar cells greatly augments neoplastic transformation by activated KRAS in a mouse model of pancreatic ductal adenocarcinoma (23). These observations imply that PTF1A is the key transcriptional regulator of pancreatic acinar cell identity.

The transcriptional activity of PTF1A requires cooperative interactions within a complex of three sequence-specific, DNA-binding proteins. In addition to PTF1A, the complex contains one

Received 22 June 2016 Returned for modification 31 July 2016

Accepted 23 September 2016

Accepted manuscript posted online 3 October 2016

Citation Hoang CQ, Hale MA, Azevedo-Pouly AC, Elsässer HP, Deering TG, Willet SG, Pan FC, Magnuson MA, Wright CVE, Swift GH, Macdonald RJ. 2016.

Transcriptional maintenance of pancreatic acinar identity, differentiation, and homeostasis by PTF1A. *Mol Cell Biol* 36:3033–3047. doi:10.1128/MCB.00358-16.

Address correspondence to Raymond J. MacDonald, raymond.macdonald@utsouthwestern.edu.

Supplemental material for this article may be found at <http://dx.doi.org/10.1128/MCB.00358-16>.

Copyright © 2016, American Society for Microbiology. All Rights Reserved.

of the common bHLH E proteins (TCF3/E12/E47, TCF4/E2.2, or TCF12/HEB) (18) and an RBP subunit, either RBPJ or RBPJL (21, 24). PTF1A and the common E protein form a heterodimer that binds an E-box (CANNTG). The heterodimer has little, if any, transactivating potential and requires an RBP subunit for its known functions (21, 25). The three-subunit complex binds DNA cooperatively; it is unable to bind a lone E-box and requires an RBP recognition sequence (TC-box; TTCCCA) spaced one, two, or three DNA turns away from an E-box (21, 26). RBPJ (RBPJ κ /CSL) is also the obligate transcription factor of the canonical vertebrate Notch signaling pathway (27, 28). The RBPJ form of the complex (PTF1-J) is required for early pancreatic development: a single-amino-acid change in PTF1A that disrupts its binding to RBPJ (but not to RBPJL) reproduces the apancreatic phenotype of the *Ptf1a*-null mouse (25).

RBPJL is the vertebrate-restricted paralog of RBPJ and is not involved in Notch signaling (21, 29). The *Rbpjl* gene is activated at the onset of acinar cell differentiation by PTF1-J (25), and the RBPJL form of the complex (PTF1-L) then drives acinar differentiation to completion (19). In mature acinar cells, PTF1-L predominates (more than 80% of PTF1A-bound sites also bind RBPJL), and the colocalization of RBPJL with PTF1A at sites in acinar chromatin signifies a functional PTF1 complex.

The regulatory scope of PTF1A in the adult has not been defined experimentally, and its presumed role in sustaining the pancreatic acinar phenotype is unproven. Here, we describe the wide range of gene control by PTF1A that maintains the specific characteristics of pancreatic acinar cell identity as well as many other properties shared by differentiated exocrine cells. PTF1A controls the pancreatic acinar transcription program by direct action at a thousand genes and in collaboration with other less cell type-restricted factors to ensure acinar cell homeostasis and to suppress other cell-type-specific programs. We discuss how the role of PTF1A in acinar cell identity relates to the pathophysiology of pancreatitis and pancreatic cancer.

MATERIALS AND METHODS

Mice. The generation of the mouse lines with the genotypes *Ptf1a*^{CreER/+} and *Ptf1a*^{fl} have been described (16, 23). *Ptf1a*^{CreER/+} has the mRNA coding region of the *Ptf1a* locus replaced with that of CreERTM (30). *Ptf1a*^{fl} has flanking *loxP* sites at kb -1.7 and $+2$ relative to the *Ptf1a* transcriptional start site; this region encompasses both *Ptf1a* exons. Details of the genomic modifications will be provided elsewhere (C. V. E. Wright, unpublished data). To inactivate the floxed allele, adult *Ptf1a*^{CreER/fl} (*Ptf1a*-cKO) mice were administered tamoxifen (TAM) at 0.25 mg/g of body weight by corn oil gavage once a day for three consecutive days. The first day of tamoxifen treatment was day 0. Control mice (*Ptf1a*^{CreER/+}) were treated in an identical manner. Pancreatic tissue samples for histology, immunofluorescence, and RNA isolation were taken after midday on days 6 and 14. The University of Texas Southwestern Institutional Animal Care and Use Committee approved all of the animal experiments.

RNA-Seq and data analysis. Total RNA was isolated from pancreas of tamoxifen-treated adult control and *Ptf1a*-cKO mice using the guanidine thiocyanate-guanidine hydrochloride method (31, 32) or a modification wherein the RNA precipitated from the initial guanidine thiocyanate homogenate was dissolved in an equal volume of TRIzol (Thermo Fisher) and then purified by following the manufacturer's protocol for a TRIzol homogenate. The average RNA integrity number values measured by an Agilent Bioanalyzer were 7.0 for the five 6-day posttamoxifen treatment *Ptf1a*^{CreER/+} mice, 7.3 for the three 6-day *Ptf1a*-cKO mice, 6.0 for the three 14-day *Ptf1a*^{CreER/+} control mice, and 6.9 for the three 14-day *Ptf1a*-cKO mice. Individual transcriptome sequencing (RNA-Seq) libraries were pre-

pared with 1 μ g of pancreatic RNA from each mouse using an Illumina TruSeq kit. Fifty-base-pair reads were collected with an Illumina HiSeq2500 instrument. The data sets for three control mice and three *Ptf1a*-cKO mice 14 days after the beginning of tamoxifen treatment have been reported previously (GEO accession number GSE70542) (23). The RNA-Seq data sets for five 6-day TAM-treated control mice (40, 42, 34, 33, and 31 million aligned reads) and three 6-day TAM-treated *Ptf1a*-cKO mice (41, 44, and 49 million aligned reads) for this study were acquired in the same manner (GEO accession number GSE86261).

The quantification of pancreatic mRNA levels by RNA-Seq is complicated by the peculiar composition of the acinar cell mRNA population. A remarkable 90 to 95% of the mRNA molecules in a pancreatic acinar cell encode fewer than 30 proteins, the secretory enzymes (33). Acini compose 85 to 90% of the mass of the pancreas (34), and therefore acinar mRNAs also dominate the total mRNA population isolated from the gland. Moreover, the amylase 2a and trypsinogen gene families have nearly identical members that account for approximately half of the total number of mRNA molecules. Changes in a single predominant mRNA, such as *Amy2a*, can compromise calculations of differential gene expression. The edgeR (35) and DESeq (36) normalization strategies correct for the computational anomalies that can arise due to these quirks in the mRNA population. Of the two, edgeR identified functionally relevant acinar genes more effectively (see Fig. S6 in the supplemental material). Proper edgeR normalization was verified by quantitative reverse transcriptase PCR (qRT-PCR) quantification of 23 mRNAs representing high- and low-abundance transcripts with large, small, or no changes in levels post-PTF1A depletion (see Fig. S2). edgeR analyses used the default TMM settings of 0.3 for trim of log ratios (M values), 0.05 for trim of combined absolute levels (A values), and an false discovery rate (FDR) cutoff of <0.05 (37). For the comparison with edgeR results, default conditions were applied for the DESeq default normalization method with the median to compute location for size factor estimation and an FDR cutoff of <0.05 (36).

The RNA-Seq analyses for four pancreases from 18.5-day-postcoitus (dpc) mouse embryos were acquired similarly (GEO accession number GSE86568), and the edgeR differential expression analysis was made with data sets from four normal C57/Bl6 adult pancreases without TAM treatment. The hierarchical cluster analysis of transcriptomes was performed using the R Stats package (38).

qRT-PCR assays were performed with SYBR green and an Applied Biosystems 2500 fast instrument. The nucleotide sequences of the primer pair that amplifies all four amylase 2a genes (pan-Amy2a) and the primer pair for four indistinguishable trypsinogen genes (pantrypsin) are provided in Fig. S2 in the supplemental material. Measurement of the ratio of spliced to unspliced *Xbp1* mRNA was performed by RT-PCR as described previously (39).

ChIP-Seq and data analysis. Preparation of mouse pancreatic chromatin immunoprecipitation (ChIP), preparation of Illumina sequencing libraries, and their analyses were performed as described previously (26), with details and modifications reported by Hale et al. (40). The antibodies are described in Table S4 in the supplemental material.

Histology, immunodetection, and image analyses. Tissue from adult mouse pancreas was prepared for histology with Carnoy's fixative (60% ethanol, 30% chloroform, 10% acetic acid). For immunodetection or lectin detection, tissue was fixed in 4% paraformaldehyde, 0.1 M sodium phosphate buffer, pH 7.4, at 4°C overnight and embedded in paraffin or cryoembedded in OCT. Table S4 in the supplemental material provides the source of antibodies and working dilutions. Micrographs are representative for three animals of each genotype-treatment combination. Samples for electron microscopy were fixed in 2.5% glutaraldehyde, 2.5% paraformaldehyde, and 0.05% picric acid in 0.1 M sodium cacodylate, pH 7.3, for 2 to 4 h at 4°C, washed extensively in 0.1 M sodium cacodylate, postfixed in 1% osmium tetroxide, dehydrated, and embedded in Epon. Thin sections were contrasted with uranyl acetate and lead citrate and examined with a Zeiss EM 109S electron microscope.

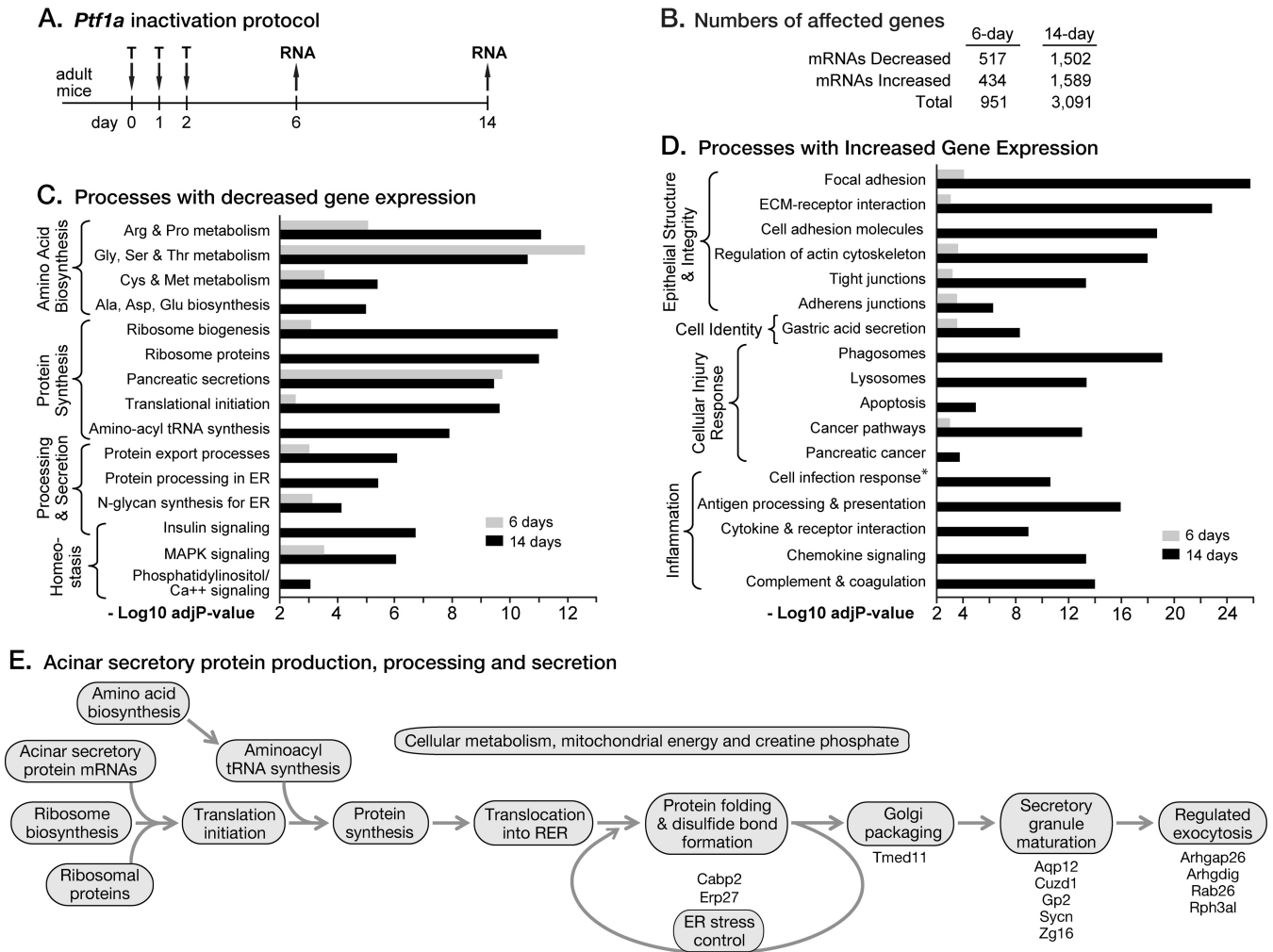


FIG 1 *Ptf1a* is required for all cellular processes for producing the acinar digestive enzymes. (A) Tamoxifen dosing scheme. (B) Differential expression analyses by edgeR of RNA-Seq quantification of mRNA changes, with an FDR cutoff of <0.05 . (C) KEGG cellular processes enriched for genes with decreased expression 6 and 14 days after initiation of tamoxifen-induced *Ptf1a* inactivation. (D) Processes enriched for genes with increased expression. The asterisk indicates the value for cell infection response pathways is the $\log_{10} P$ value average ($-\text{Log}_{10} \text{adjP-value}$) of seven KEGG pathways for cellular infection. (E) All processes in the production pathway for digestive enzymes were adversely affected. Newly identified or understudied acinar cell-restricted genes are listed beside their cellular process.

Acinar cells depleted of PTF1A were lineage traced by tamoxifen-induced CreER-mediated recombination of the *Rosa-CAG-LSL-tdTomato* locus (MGI:3809524) (41) in *Ptf1a^{CreER/+}* and *Ptf1a^{CreER/fl}* mice. Cell type expression of tdTomato was determined by coimmunofluorescent staining for tdTOM and acinar and ductal markers with pancreases 6 and 14 days after tamoxifen initiation.

The mean circumference of acinar cells was quantified with ImageJ. Approximately 200 cells were measured for each of three animals of each genotype and treatment. Acinar cells were identified by clear apical-basal organization and with an apex facing a lumen, as revealed by E-cadherin and laminin immunostaining. The frequency of apoptotic cells was quantified from the number of cells staining with the antibody to the activated form of caspase 3 in a $5\times$ microscopic field and corrected for the increased cell density of the *Ptf1a*-cKO pancreatic tissue, measured with the aid of ImageJ. All values are expressed as means \pm standard deviations (SD). Statistical analyses were performed using a 2-tailed Student unpaired *t* test. A *P* value of <0.05 was used to exclude the null hypothesis.

Accession numbers. RNA-Seq and ChIP-Seq data sets determined in the course of this work were deposited in the GEO database under accession numbers GSE86261, GSE86262, and GSE86568.

RESULTS

To examine the effects of PTF1A depletion on adult acinar gene expression and homeostasis, we used *Ptf1a*-cKO mice, with the coding sequence of one *Ptf1a* allele replaced by that of CreER (*Ptf1a^{CreER}*) (16) and the other allele flanked by *loxP* sites (*Ptf1a^{fl}*) (23). Adult *Ptf1a*-cKO mice and age-matched heterozygous control mice (*Ptf1a^{+/CreER}*) were treated with tamoxifen to inactivate the floxed allele, and RNA was isolated from pancreases 6 or 14 days after the onset of the treatment (Fig. 1A). The extent of deletion of *Ptf1a* by two measures was 87 to 97% (see Fig. S1 in the supplemental material). Analysis of changes in the mRNA population by RNA-Seq at 6 days was chosen to detect early effects of PTF1A depletion and at 14 days to confirm gene expression changes and to examine the secondary effects of prolonged depletion. The highly unusual composition of the pancreatic mRNA population requires a rigorous RNA-Seq normalization strategy such as edgeR (see Materials and Methods). Requantification using qRT-PCR of 23 mRNAs representing high- and low-

abundance transcripts with large, small, or no changes after *Ptf1a* inactivation verified the edgeR-calculated RNA-Seq values of differential expression (see Fig. S2).

The sets of genes with decreased mRNA levels in *Ptf1a*-cKO pancreas at 6 days (518 genes) and 14 days (1,508 genes) (Fig. 1B; see also Table S1 in the supplemental material) were greatly enriched in cellular pathways for the production of large amounts of the digestive enzymes, especially synthesis, processing, packaging, and secretion, as well as the regulation of those processes (Fig. 1C and E). In contrast, genes with increased mRNA after *Ptf1a* inactivation (434 at 6 days, 1,586 at 14 days) were more often associated with cellular stress, acinar epithelial integrity, and inflammation (Fig. 1D). The genes of these categories were generally induced in response to the disruption, evident at 6 days, of many critical acinar functions. Because acinar cells dominate the composition of the pancreas and have severalfold higher levels of mRNA per cell than islet or duct cells, major changes in mRNA levels derive from acinar cells; we verified key examples by cell type-based immunofluorescence analyses. The mRNAs for marker genes of the endocrine pancreas (insulin 1 and 2, glucagon, somatostatin, ghrelin, and pancreatic polypeptide) did not change.

To illustrate the breadth and depth of the direct regulatory responsibilities of PTF1A, we describe the effect of PTF1A depletion on vital acinar cell processes and the subsequent PTF1A-independent induction of homeostatic and pathological responses. We previously reported the effects of *Ptf1a*-cKO at 14 days (23); at this late stage, secondary effects of PTF1A loss predominate. In the current study, we use the 14-day results to distinguish secondary (indirect) effects from primary (direct) effects of PTF1A depletion on gene expression evident at 6 days and to confirm early trends.

Decreased acinar cell differentiation. The mRNAs for 27 of 30 hallmark secretory digestive enzymes and cofactors decreased at 6 days (29 at 14 days) by as much as 96% (Fig. 2A and B). All but four of the affected genes have PTF1A bound to regulatory sequences, as shown by the coassociation of PTF1A with RNA polymerase II (RNAPII) and the transcriptional activation mark H3K4me2 by ChIP-Seq analyses (e.g., *Cpa1*) (Fig. 2I). Because the PTF1A-E protein heterodimer does not have transcriptional activity, we also show the presence of RBPJL, the predominant RBP subunit of the functional PTF1 complex in adult acinar cells. Here, we use the term “direct target” for genes with PTF1A bound (associated using GREAT [42]) and with decreased mRNA early (at 6 days), suggestive of an acute effect of PTF1A depletion. Genes for the support mechanisms for the prodigious protein synthesis were also affected by the inactivation of *Ptf1a*, including genes for 14 amino acid transporters, biosynthetic enzymes for 9 of the 10 non-essential amino acids, and components for ribosome biosynthesis, including 22 of the 78 ribosomal proteins, 11 of the 31 tRNA charging enzymes, and 13 translation-initiation factors (see Table S2 and Fig. S3A in the supplemental material), as well as the gene for mTOR-controlled translational regulator EIF4EBP (Fig. 2J). In addition, genes of the AKT/MTOR pathway, which controls many aspects of acinar protein synthesis and growth (43), were misregulated (see Fig. S4).

This analysis of the pancreatic mRNA population indicated that PTF1-deficient acinar cells lost the ability to produce large amounts of the secretory enzyme mRNAs. This led to greatly reduced secretory enzyme stores and much smaller acinar cells. The

decrease of carboxypeptidase A1 (*Cpa1*) mRNA was representative of most of the secretory protein mRNAs (Fig. 2). CPA1 protein was partly depleted at 6 days and nearly absent from most acinar cells by 14 days (Fig. 2E to G). Cells that retained normal levels of CPA1 had escaped inactivation of *Ptf1a* (see Fig. S1 in the supplemental material); thus, the effects of PTF1A depletion were cell autonomous, and CPA1 is an effective proxy for PTF1A. Not all acinar secretory protein genes were affected equally. For example, amylase mRNA (Fig. 2C) and protein levels (Fig. 2H) were affected much less by the status of PTF1A, which illustrates the range of dependence of secretory protein gene expression on PTF1A. By 14 days, the PTF1A-depleted cells had shrunk to about one-eighth their normal volume (Fig. 2D).

Genes for the high-capacity intracellular processing of secretory protein were also affected early, including those encoding proteins of signal peptide recognition, cleavage, and protein import into the rough endoplasmic reticulum (RER), protein folding and disulfide bond formation, monitoring protein folding with N-glycan registration, ER stress control, protein transport to the Golgi complex, and packaging into and maturation of zymogen granules (Fig. 3A and B). Decreased expression for at least 66% of these genes is due to direct PTF1A control (asterisks). For example, AQP12 is the intracellular water pump that concentrates secretory proteins during passage to and within zymogen granules (44). Its mRNA decreased to 24% by 6 days, and PTF1A and RBPJL bind a control region occupied by RNAPII and methylated H3K4 near its transcriptional start site (Fig. 2K). We identified 12 understudied acinar target genes based on their high, pancreas-restricted expression and strong decrease after PTF1A depletion (Fig. 3E). Each appears to enhance a potential rate-limiting step in secretory protein production and to be a direct PTF1A target (e.g., *Cabp2*) (Fig. 3M).

Altered expression of genes for ER functions, ER-associated degradation (ERAD), and autophagy (see below) indicated that PTF1A-deficient acinar cells undergo ER stress from the accumulation of unfolded secretory protein. The status of the unfolded protein response (UPR) can be estimated by the ratio of spliced to unspliced cytoplasmic mRNA for XBP1 (39), which is a key transcriptional activator of UPR genes. In control mice, the ratio in the pancreas was 2.5:1 (Fig. 3C). Despite decreased secretory protein mRNA levels, the UPR was further induced after *Ptf1a* inactivation, coincident with the lost expression of ER chaperones, disulfide isomerases that assist folding, regulators of the UPR, and ERAD proteins (Fig. 3B). Genes with decreased mRNAs for key components of these processes (e.g., *Sell1* for ERAD and *Atf6* for UPR control) are direct targets of PTF1A (Fig. 3N and O). The spliced to unspliced ratio was doubled by 6 days and more than doubled again at 14 days (Fig. 3C). With increasing ER stress, ER chaperones and components of ERAD not dependent on PTF1A were then induced at 14 days, as were six known pancreatic stress response proteins (Fig. 3D). The level of the stress protein clusterin increased in PTF1A-deficient cells as early as 6 days later (Fig. 3F to H). With the stress response compromised, the mRNAs of apoptotic initiators rose (Fig. 3B) and the frequency of apoptotic cells (staining for activated caspase 3) increased 16-fold (Fig. 3I to L).

To examine the broad changes of acinar cell differentiation, we compared the transcriptomes of control pancreas, pancreas after *Ptf1a* inactivation, and late-stage prenatal (embryonic day 18.5 [E18.5]) pancreas. The gene expression profile at 14 days of

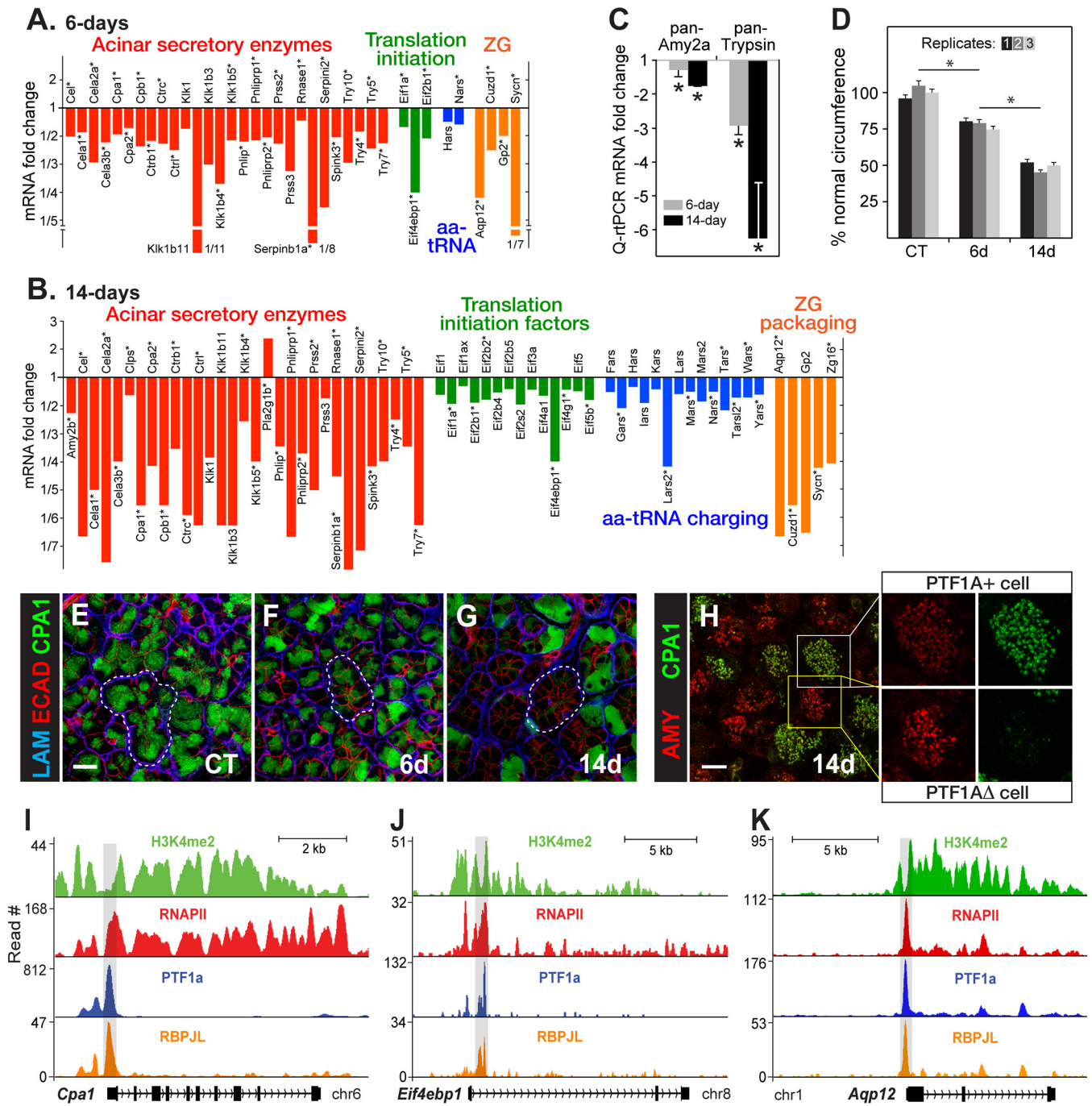


FIG 2 Loss of acinar cell differentiation: manufacture of secretory proteins. (A and B) Fold changes in the expression of genes for *Ptf1a*-cKO at 6 and 14 days relative to control TAM-treated, *Ptf1a*^{+/*CreER*} pancreases. Asterisks indicate genes with bound PTF1A in pancreatic chromatin. (C) qRT-PCR measurements of total amylase or trypsinogen mRNAs ($n = 3$; $P < 0.05$). (D) Measurements of the circumference of acinar cells. $P < 0.05$. CT, control. (E to G) Laminin, E-cadherin, and CPA1. Outlined regions are examples of acini. Scale bar, 20 μm . (H) Higher-magnification immunostaining of amylase and CPA1 after PTF1A depletion. Bar, 10 μm . (I to K) PTF1A binding to representative direct target loci occurs at sites with markers of active enhancers (RNA polymerase 2, RNAPII; histone3-lysine4-dimethylation, H3K4me2) and the coassociation of the PTF1A cofactor RBPJL (shaded regions). The shaded region of *Cpa1* is an enhancer with pancreatic acinar specificity in transgenic mouse assays (26).

PTF1A depletion was more similar to that of the prenatal pancreas than to that of control adult pancreas (Fig. 4A). The status at 6 days was intermediate between the control and 14-day pancreases, indicating a decline in differentiation as PTF1A diminished and secondary effects accrued. Fifty-one percent of the mRNAs that

decreased after depletion of PTF1A in the mature pancreas increased during normal postnatal maturation (Fig. 4B). These changes involved cellular processes characteristic of the differentiated acinar phenotype: the synthesis, processing, intracellular transport, and secretion of the digestive enzymes (Fig. 4C). Other

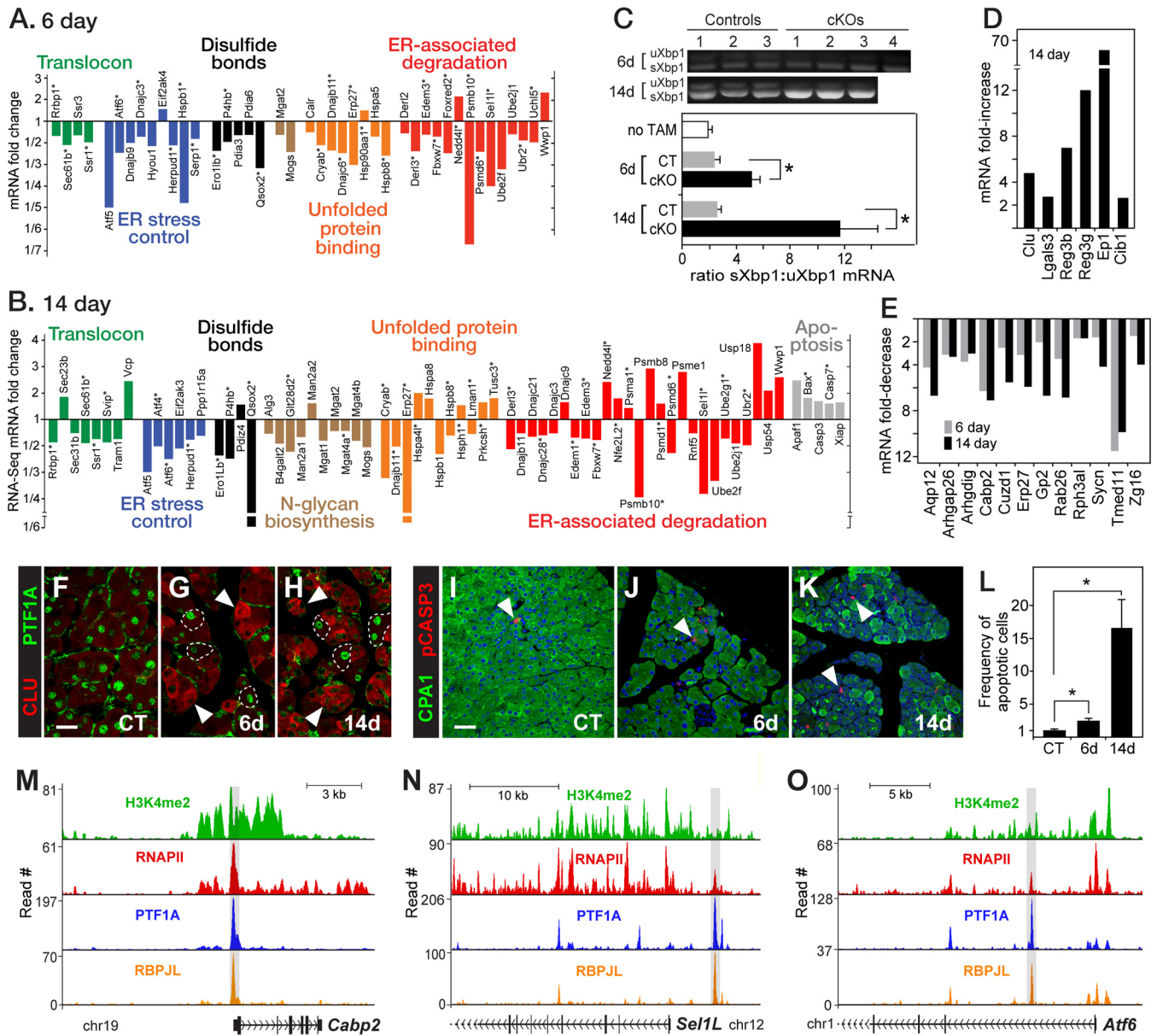


FIG 3 Loss of PTF1A disrupts the expression of genes for protein processing, packaging, and secretion, and it induces ER stress. (A and B) Changes in the expression of genes for the import of secretory protein into the RER, folding with disulfide bond formation, monitoring folding and ER stress control, ERAD, and apoptosis. (C) Quantification of the ratio of spliced to unspliced Xbp1 mRNA ($n = 3$ or 4 for each condition; *, $P < 0.05$). (D) Induction of the mRNAs of pancreatic stress proteins at 14 days; all FDR cutoffs were $< 10^{-8}$. (E) Decreased expression of newly identified or understudied genes highly expressed and largely restricted to the pancreas; all FDR cutoffs were $< 10^{-6}$, except for *Rph3al* (0.004). (F to H) Induction of clusterin (CLU) in acinar cells that lost PTF1A (arrowheads, examples of CLU⁺ cells; dashed lines, cells with PTF1A that do not stain for CLU; bar, 20 μ m). (I to K) Increase of apoptotic cells (arrowheads) with activated caspase 3. Bar, 40 μ m. (L) Relative number of apoptotic cells per field, corrected for cell density ($n = 3$ for each genotype/treatment; *, $P < 0.05$). (M to O) PTF1A binding in association with H3K4me2, RNAPII, and RBPJL at *Capb2*, *Sell1*, and *Atf6*.

features of acinar differentiation, such as specific aspects of energy metabolism, were unaffected by the loss of PTF1A (Fig. 4D). Despite the decrease of the differentiation properties that define the acinar phenotype, inactivation of *Ptf1a* did not reactivate embryonic genes representative of an early pancreatic progenitor cell status (e.g., *Pdx1*, *Prox1*, and *Nkx6.1*).

Alteration of acinar cell identity. To evaluate qualitative changes of differentiation, we asked whether mutant acinar cells induced genes characteristic of other cell types. Because pancre-

atic injury can cause acinar cells to acquire ductal properties, a process termed acinar-to-ductal metaplasia (ADM), we examined whether the often-used ductal markers SOX9 and cytokeratin-19/KRT19 appeared. *Sox9* mRNA increased 2.8- and 4.6-fold at 6 and 14 days after *Ptf1a* inactivation, respectively (Fig. 5A), whereas the *Krt19* mRNA level did not change. SOX9 and KRT19 are readily detected in pancreatic duct cells and the duct-like centroacinar cells but also are present in mature acinar cells at very low (16) and often undetectable levels (Fig. 5D and G). By our analysis, SOX9

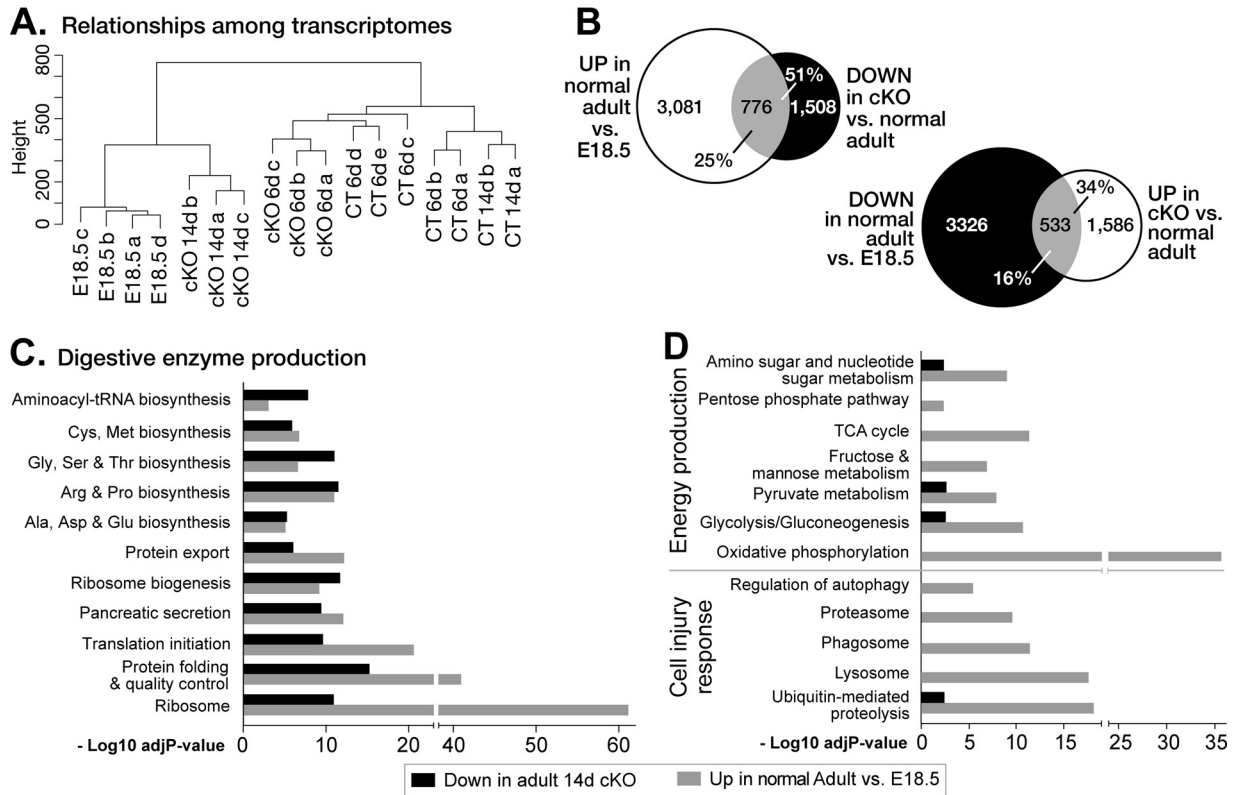


FIG 4 *Ptf1a* maintains acinar differentiation. (A) Cluster analysis of the relationships among the gene expression patterns of TAM-treated normal adult (CT), *Ptf1a*-cKO adults after 6 and 14 days, and untreated E18.5 fetal mouse pancreases. (B) Gene expression changes during the last stage of acinar differentiation (E18.5 to normal adult) and in response to PTF1A depletion in adult (*Ptf1A*-cKO at 14 days versus CT). The number of genes affected and the percentage of genes in the overlap for each category are shown. (C) Similar cellular pathways are enriched with genes downregulated after PTF1A depletion (down in adult 14-day cKO mice) and with increased expression during the postnatal stage of pancreatic differentiation (higher in adult versus E18.5 pancreases). (D) Divergent effects for pathways of energy production and responses to cell injury. TCA, tricarboxylic acid.

and KRT19 proteins appeared in PTF1A-deficient acinar cells as early as after 6 days and were prevalent at 14 days (Fig. 5E, F, H, and I). The induction of KRT19 must be controlled principally posttranscriptionally. Other instructive ductal markers, HNF1B and HNF6, did not change.

This rapid acquisition of ductal markers is a direct response to the depletion of PTF1A rather than to cumulative and progressive changes in response to pathologies over time. Several lines of evidence indicate that the SOX9/KRT19-positive duct-like cells formed by conversion of acini rather than expansion of ducts: the change was rapid, and intermediate ADM structures marked by residual CPA1 and amylase were readily apparent; ductal cell replication did not increase, and there was insufficient acinar cell apoptosis to allow an increased proportion of duct-like cells via the death of acinar cells. Moreover, lineage tracing of acinar cells by TAM-induced Rosa-CAG-LSL-TdT activation in *Ptf1a*-cKO pancreas demonstrated that the new CK19(+) and SOX9(+) derived from acinar cells (see Fig. S1 in the supplemental material).

More striking was the predominance of known stomach-specific markers among the mRNAs, with the greatest increases after 14 days of PTF1A depletion. Half of the 28 genes with the highest induction ratios (see Table S3 in the supplemental material) were highly expressed differentiation markers of the major epithelial cell types of the gastric gland: mucous, parietal, or chief cells (Fig. 5A). MUC5AC is an acidic mucin of the pit/tip cells, and CHIA1 is

a digestive enzyme of chief cells (Fig. 5J). *Chia1* mRNA was induced 47- and 97-fold at days 6 and 14 in *Ptf1a*-cKO pancreas, and CHIA1 protein appeared in the PTF1A-depleted acinar cells (compare Fig. 5B and C). Most of these gastric genes are not normally expressed in pancreatic ducts. In contrast, we found that KRT19, SOX9, and CAR2, routinely considered ductal markers, are present at high levels in the glandular stomach (Fig. 5J). KRT19 is in the MUC5AC-positive mucous tip/pit cells. SOX9 is in cells of the neck region (45, 46) that overlap GSII-stained mucous cells and a subset of Ki67-positive progenitor cells of the isthmus (47). CAR2 is in the acid-secreting parietal cells. The ambiguity of the ductal markers, the absence of induction of more instructive ductal markers such as HNF1B or HNF6, and the large number of induced gastric markers suggest that the change in acinar cell identity involves the acquisition of aspects of gastric rather than pancreatic ductal identity.

MECOM (EVI1/PRDM3) is a DNA-binding transcription factor partly restricted to the glandular stomach and linked to the transcription of five of the gastric gland-restricted genes (*Gif*, *Kcne2*, *Chia*, *Pga5*, and *Pgc*) (48) induced after PTF1A depletion. These five gastric mRNAs were increased in the pancreas 6 days after *Ptf1a* inactivation, when *Mecom* mRNA levels had risen 3.8-fold (see Fig. 7B). Other gastric genes without detectable mRNA in the normal pancreas were activated after 14 days, when *Mecom* expression had increased further. Whereas the

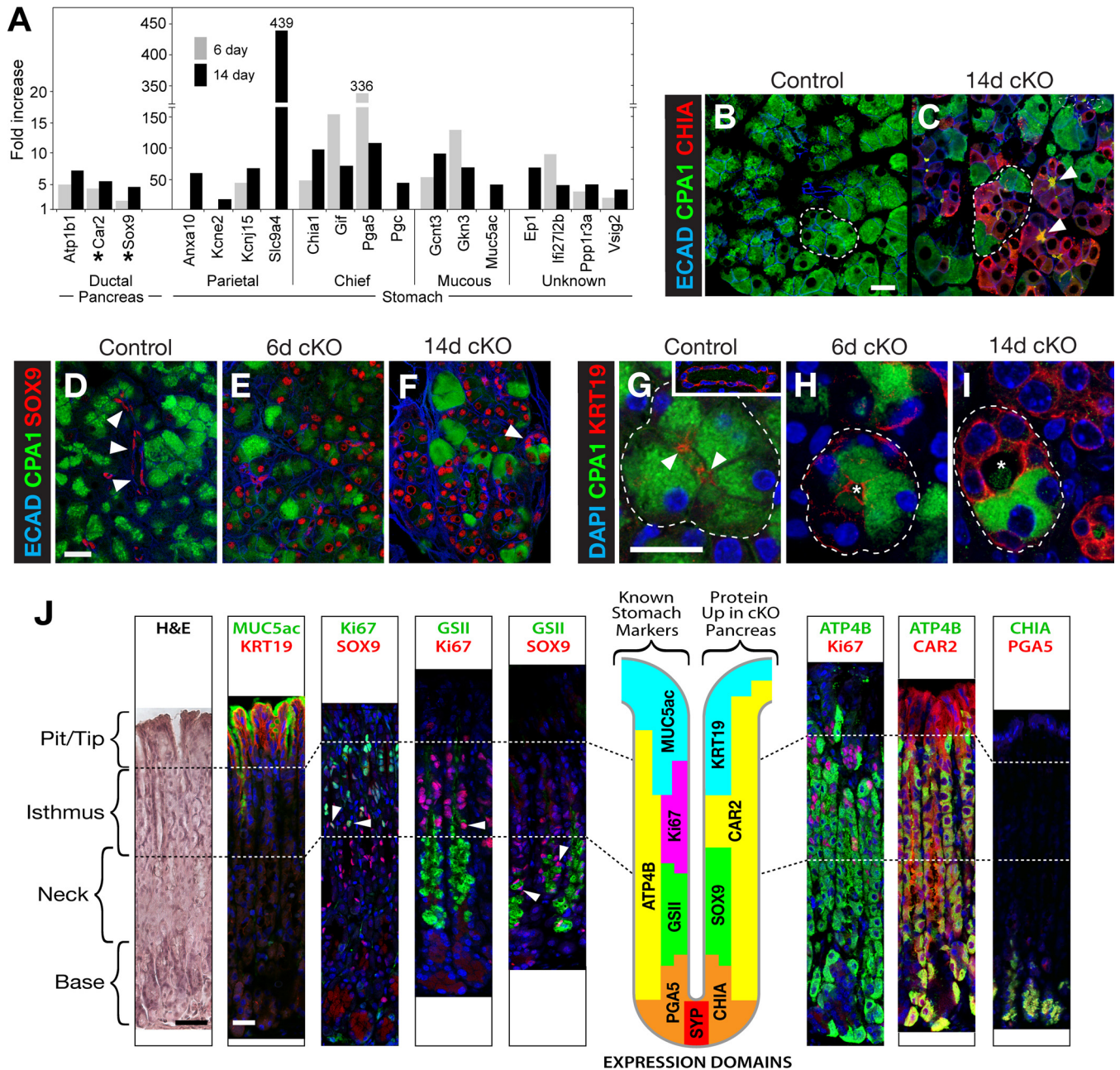


FIG 5 Acinar cells acquire ductal and gastric markers. (A) RNA-Seq quantification of mRNAs for markers of pancreatic duct cells and epithelial cell types of the stomach. Asterisks indicate genes expressed in ductal pancreas as well as stomach. (B to I) Ductal and gastric markers appear in acinar cells that lose CPA1 (i.e., PTF1A deficient) but not in cells that retain CPA1. (B and C) CHIA is readily detected in CPA1-depleted acinar cells (arrowheads indicate intense secreted CHIA and CPA1 in ductules). Outlined regions are examples of a homogenous acinus (B) and a mixed acinus (C). Bar, 20 μ m. (D to F) SOX9 in CPA1-depleted acinar cells (arrowheads in panel D, SOX9⁺ small duct; arrowhead in panel F, hybrid acinus). (G to I) KRT19 (arrowheads in panel G indicate KRT19⁺ centroacinar cells; asterisks in panels H and I indicate lumina). (J) Gastric genes induced in Ptf1a-cKO acinar cells. Arrowheads indicate examples of cells with colocalization of Ki67/SOX9, Ki67/GSII⁺ mucin, or SOX9/GSII⁺ mucin. GSII is a fluorescein-conjugated lectin specific to a mucin of neck mucous cells. Bars, 40 μ m. The diagram of a gastric gland illustrates the expression domains of known gastric markers (left; all but ATP4B and the unknown mucin target of GSII were induced in Ptf1a-cKO pancreas) and additional gastric/ductal proteins induced in Ptf1a-cKO acinar cells (right). H&E, hematoxylin and eosin.

early-induced gastric genes had PTF1A and RBPJL bound at prospective control regions and RNAPII and methylated H3K4 at transcribed regions in normal acinar cells, the gastric genes induced late did not (data not shown). Thus, the late gastric genes appeared to be activated *de novo* after PTF1A depletion, as *Mecom* reached a threshold.

Acinar cell degeneration is a delayed consequence of *Ptf1a* inactivation. The inability to respond effectively to stress in the wake of sudden loss of PTF1A led to acinar cell injury and increased cell death. The insulin, RTK/RAS/mitogen-activated protein kinase (MAPK), and phosphatidylinositol 3/calcium signaling pathways maintain the physiologic tone of acinar cells

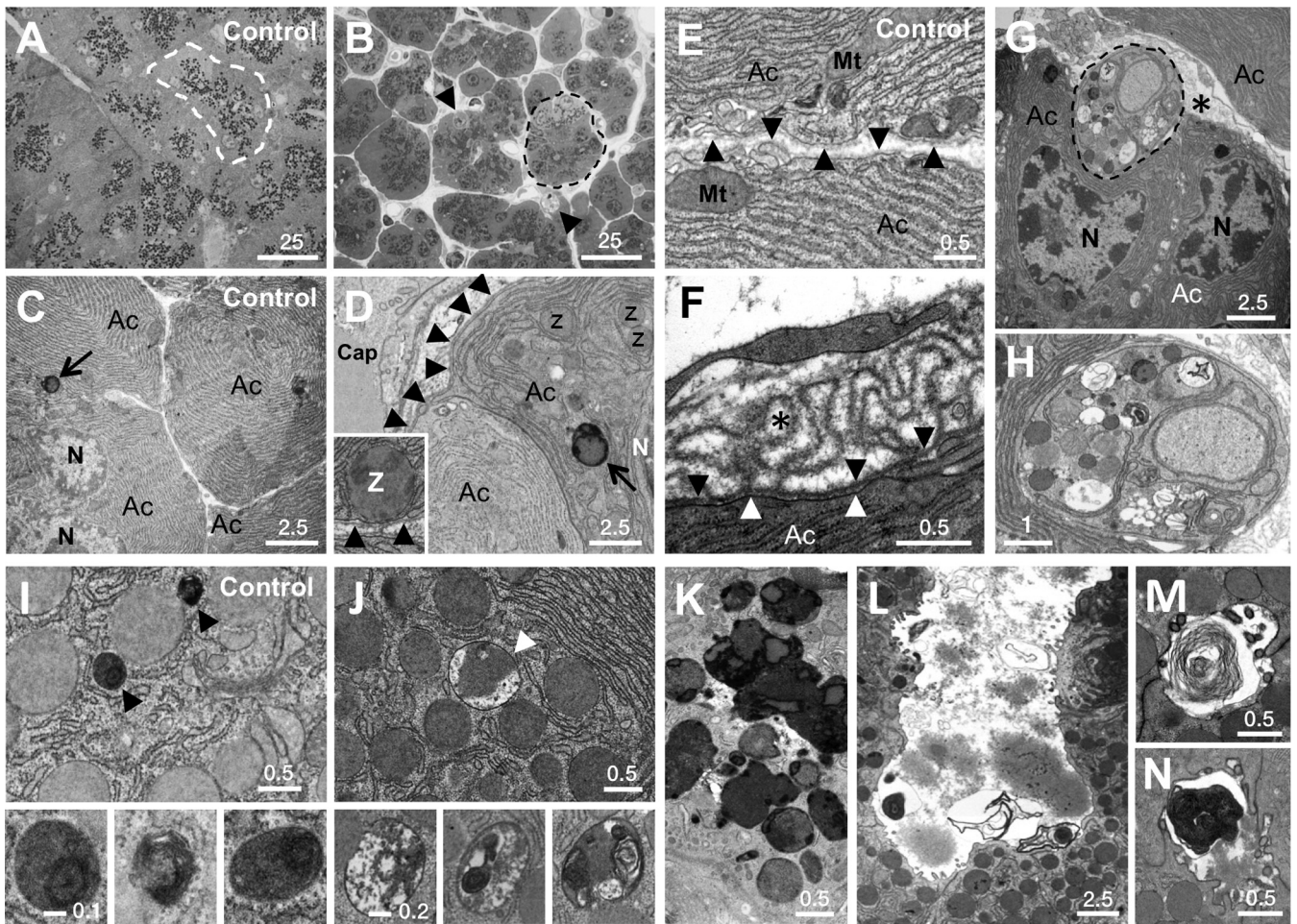


FIG 6 Ultrastructural changes in PTF1A-deficient pancreas. All panels are of 14-day cKO mice except for TAM-treated *Ptf1a*^{+/CreER} controls in panels A, C, E, and I. (A to D) Effects on apical-basal polarity; dashed lines outline individual acini. Zymogen granules (dark dots), normally clustered apically around lumina (A), are decentralized in cKO pancreas (B; arrowheads indicate phagosomes). Zymogen granules, rarely basal to nuclei (C), are basal in cKO pancreas (D). The inset shows zymogen granule apposed to basal plasmalemma. Arrowheads, basal lamina; arrows, lysosomes. (E and F) Excessive basal lamina (asterisk) of a shrunken acinar cell (F) compared to normal acinar cells (E). Black arrowheads indicate basal lamina from which folds emanate; white arrowheads indicate basal plasmalemma. (G) Phagocytic engulfment by acinar cells (dashed outline in panels B and G). (H) Thin band of cytoplasm bounded by plasmalemma is enlarged. (I) Zymogen granules and lysosomes (arrowheads) in control cells. Insets show enlarged lysosome images. (J) Crinophagic vesicles (arrowhead) are the size of zymogen granules. Insets show complex interior structures. (K) Extensive crinophagic fusions. (L to N) Frequent luminal debris, including lamellar membranes. Size bar length units are micrometers. Ac, acinar cell; Cap, capillary; Mt, mitochondrion; N, nucleus; Z, zymogen granule.

(49–51). Each of these pathways was enriched for genes affected early by the loss of PTF1A (see Fig. S3A in the supplemental material). The output of the RAS/MAPK pathway, measured by the level of phosphorylated RPS6, decreased in PTF1A-depleted acinar cells coincident with the induction of the stress protein clusterin (see Fig. S4B and C). Changes also occurred in the Notch and Wnt pathways (see Fig. S3A), which are necessary for acinar cell regeneration after injury (52, 53). Increased mRNAs for components of the adherens and tight junctions, extracellular matrix, and cellular adhesion (see Fig. S3B) suggest induced repair of epithelial structure and integrity. Apical-basal polarity was also affected: zymogen granules, normally positioned apically around a central lumen (Fig. 6A), were more evenly distributed throughout cells of an acinus (Fig. 6B) and were even present between the plasmalemma and the nucleus in the basal region normally occupied by RER (compare Fig. 6C and D). Acinar cell shrinkage (Fig. 2D) led to folded sheets of excess basal lamina (compare Fig. 6E

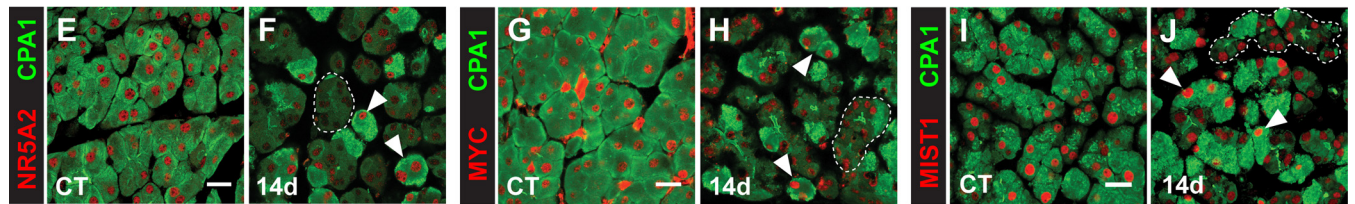
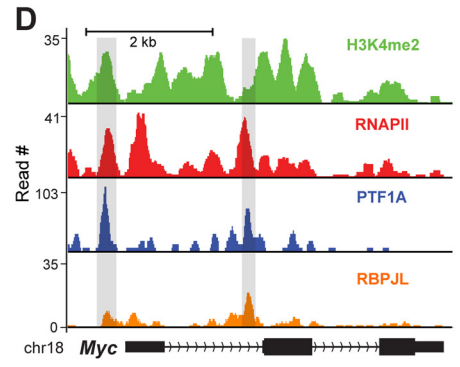
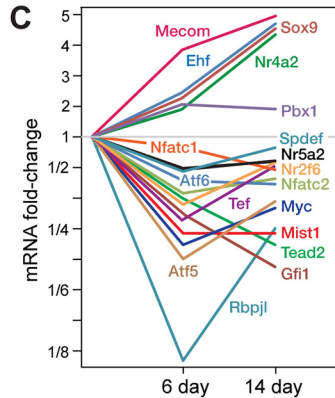
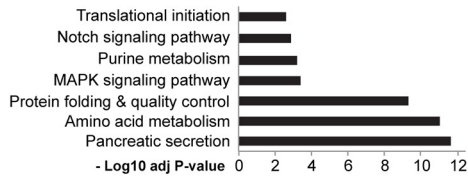
and F); an induced repair process (54) may account for the increased mRNAs for extracellular matrix components detected in the *Ptf1a*-cKO pancreas (see Fig. S5A).

Genes of the cellular response to injury, including intracellular degradation pathways and inflammation, were induced during the second week of PTF1A depletion (see Fig. S3B in the supplemental material), influencing autophagy, highly unusual phagocytosis of acinar cells by acinar cells (Fig. 6G and H), and crinophagy in most affected acinar cells (Fig. 6J). Crinophagic vacuoles can be distinguished by size (similar to zymogen granules and much larger than lysosomes), high and heterogeneous electron density, and the absence of membranous substructure (compare insets of Fig. 6I and J). Extensive crinophagy (e.g., Fig. 6K) is a protective mechanism that degrades excess, potentially harmful accumulated secretory products during stress (55). In addition, unusual and excessive collections of cell fragments in acinar and ductal lumina, including membrane-bound structures similar to

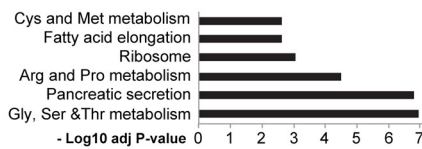
A. PTF1A direct targets

# PTF1A sites	# associated genes	
9,515	7,210	
Activated genes	Repressed genes	Total
337 (62%)	208 (38%)	545

B. PTF1A-bound and activated genes



K. NR5A2-activated Ptf1a-target genes



L. Myc-dependent Ptf1a-target genes

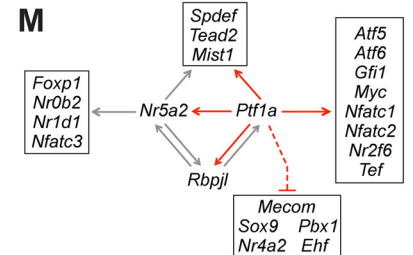
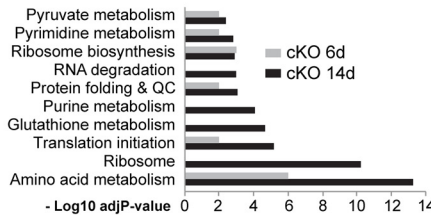


FIG 7 PTF1A transcription factor network. (A) Number of PTF1A direct targets. Shown are genes associated with PTF1A-bound sites and with mRNA levels affected at both 6 and 14 days after *Ptf1a* inactivation. (B) Functional classifications of PTF1A direct targets that require PTF1A. (C) Kinetics of changes for mRNAs of TFs affected by PTF1A depletion. (D) PTF1A, RBPJL, and active chromatin marks colocalize at *Myc*. (E to J) Loss of NR5A2 (E and F), MYC (G and H), and MIST1 (I and J) in CPA1-deficient cells but retention in CPA1⁺ cells compared to controls (CT). CPA1 is an effective measure of *Ptf1a* status (see Fig. S1 in the supplemental material). Outlined regions indicate acini with loss of CPA1; arrowheads indicate acinar cells retaining CPA1 and NR5A2, MYC, or MIST1. Bars, 20 μ m. (K) Functional classifications of the NR5A2-dependent genes that are also PTF1A dependent. (L) Functional classifications of MYC-dependent genes (by IPA; Qiagen) that are also PTF1A dependent. (M) Proven direct interactions of the Ptf1a transcription factor network. Red lines and arrows are from data from this study; the dashed line indicates that repression may be indirect.

those that arise during cerulein-induced inflammatory pancreatitis (56), suggest the expulsion of acinar cell debris apically or lysis of whole cells (Fig. 6L to N). The spectrum of acinar cell lesions was accompanied by increased mRNA levels of inflammatory genes, such as those for components of complement, cytokines, and chemokines in acinar cells as well as activated pancreatic stellate cells (57) (see Fig. S5B) but without the increased numbers of CD45⁺ leukocytes that would indicate frank inflammation (data not shown).

The presence in acinar cells of Ki67, which indicates an active cell cycle, differed from the cell-autonomous status of *Ptf1a*. Whereas the PTF1A-deficient acinar cells at day 14 had Ki67 at about the same frequency (0.22% \pm 0.13% standard deviations) as acinar cells of normal C57Bl6 and TAM-treated control mice (0.27% \pm 0.17%), the frequency of Ki67 in the residual PTF1A-positive acinar cells of the cKO pancreas was ~60-fold greater (16% \pm 2%). The induction of the cell cycle in PTF1A⁺ cells correlates with partial regeneration of the acinar tissue. At 29 weeks after TAM treatment, the weight of the cKO pancreas was 67% of normal (see Fig. S5C in the supplemental material), largely

due to the restoration of CPA1 and PTF1A copositive acinar cells (see Fig. S5D and E), presumably from restorative replication of those acinar cells that avoided *Ptf1a* inactivation. Dispersed PTF1A-deficient regions of tubular complexes expressing SOX9 and gastric mucin persisted (see Fig. S5D and E).

The PTF1A transcription factor network. To better assess direct regulatory control by PTF1A binding to potential target genes, we examined genome-wide binding of PTF1A in chromatin from adult acinar cells using four independent ChIP-Seq data sets, two from each of two independently derived PTF1A antibodies. Analysis using Homer identified 9,515 genomic sites with bound PTF1A present in all four data sets, associated with 7,210 genes (Fig. 7A). A total of 545 genes were both bound and regulated by PTF1A. Genes dependent on PTF1A were associated with pathways for acinus-specific cell functions (Fig. 7B). Those induced by the loss of PTF1A were still enriched for gastric genes (not shown).

Thirteen additional acinar transcription factors are bound by and dependent on PTF1A (Fig. 7C). The expression of each decreased 26 to 78% after *Ptf1a* inactivation, and PTF1A and RBPJL

bound their genes at sites also colocalized with RNAPII and H3K4me2 (Fig. 7D and data not shown). Consistent with changes in mRNA levels, NR5A2, MYC, and MIST1 diminished in the PTF1A-depleted acinar cells but not in the small fraction of cells that retained PTF1A (Fig. 7E to J). *Ptf1a*, *Rbpjl*, *Nr5a2*, *Myc*, and *Mist1* have specialized acinar cell functions and extensive cross-regulation, and they appear to form the core of the gene regulatory network. NR5A2 binds and regulates the genes of four members of the network: *Rbpjl*, *Mist1*, *Tead2*, and *Spdef* (40, 58). Moreover, half of the genes downregulated in adult *Nr5a2*-cKO pancreas (223/452) (58) were also reduced by *Ptf1a* inactivation and enriched for acinus-enhanced functions and cell-specific products (Fig. 7K). Similarly, 118 MYC-dependent genes (according to Ingenuity pathway analysis [IPA]; Qiagen) expressed in the pancreas are also bound by and dependent on PTF1A. MYC enhances protein synthetic capacity by activating genes for ribosomal proteins and rRNA processing (e.g., *Nop56*, *Bop1*, and *Dkc1*) (59) and stimulates protein synthesis rates through genes for initiation factors (e.g., *Eif2b1*, *Eif2b4*, *Eif2s2*, *Eif1a*, and *Eif4g1*) (see Table S1 in the supplemental material), key acinar genes and functions also affected by *Ptf1a* inactivation (Fig. 7L). Several MIST1 target genes, including *Rab3d*, *Ccpg1*, *Serpini1*, *Reg1*, *Nupr1*, and *Rab26* (60), are coregulated directly by PTF1A.

The other members of the network (SPDEF, TEAD2, GF11, ATF6, TEF, NFATC1, and NFATC2) are partially cell type restricted, although not as selectively to pancreatic acinar cells as PTF1A and RBPJL; all have roles in differentiation, growth, metaplasia, or transformation (see Discussion). Increased mRNA levels of the TF genes *Mecom*, *Sox9*, *Pbx1*, *Nr4a2*, and *Ehf* in PTF1A-deficient pancreas (Fig. 7C) indicate that PTF1A suppresses their expression. However, binding to these genes is low and may account for the low level of expression in normal pancreas. Consistent with activation, H3K4me2 and RNAPII are present. Other transcriptional activators might mediate the induction in the absence of PTF1A.

DISCUSSION

Pleiotropic control of the pancreatic acinar phenotype. Our analysis of the effects of PTF1A depletion shows that PTF1A has comprehensive regulatory duties that maintain the differentiated phenotype of the pancreatic acinar cell by controlling genes of all the major processes for the massive production of secretory digestive enzymes. PTF1A accomplishes this from the top of a transcriptional regulatory hierarchy that drives specialized genes restricted to pancreatic acinar cells (e.g., the pancreatic secretory proteins), others of the less restricted class of professional secretory cells (e.g., secretory protein processing and packaging), and specialized enhancements of broadly expressed genes (e.g., enzymes of amino acid metabolism, ribosomal proteins, and translation initiation factors) in support of secretory enzyme production. The control of gene expression is direct, by binding and transcriptional activation of many acinar genes, and also indirect, through the direct control of other TFs enriched in acinar cells. These other pancreatic transcriptional regulators have important but limited regulatory roles in acinar cells. The effects of their absence during late development (i.e., *Mist1* or *Rbpjl*) or induced depletion in the adult (*Nr5a2*) are modest (19, 58, 60) and limited to loss of some differentiation characteristics but retention of cell identity.

The initial effects of *Ptf1a* inactivation are principally at PTF1A

target genes, including those for acinar secretory enzymes and their processing and packaging partners in the endoplasmic reticulum, as well as many ER components for secretory protein folding and quality control. The early effects include reduced expression of several genes notable for high mRNA levels and highly restricted expression that boost the capacity of protein folding in the ER (*Erp27* and *Cabp2*), direct transport to the Golgi complex (*Tmed11*), concentrate secretory proteins in the Golgi complex and condensing zymogen granules (*Aqp12*), organize the packaging of the secretory proteins (*Gp2*, *Sycn*, *Cuzd1*, and *Zg16*), and promote the proper organization of the apical cytoplasm (*Rab26*) (61). These gene expression defects establish the conditions for the subsequent disruption of cellular homeostasis. Due to the vast production of secretory proteins, pancreatic acinar cells normally have a chronically high level of unfolded protein and a precarious homeostasis (62, 63). We find that after *Ptf1a* inactivation, the contribution of secretory protein mRNAs to the total mRNA population declines from 90% to about 55%. This fraction can still support an enormous amount of secretory protein synthesis. The sudden disappearance of PTF1A creates an imbalance between the continued production of secretory proteins and the decaying capacity of the ER to process or degrade unfolded proteins, and ER stress increases further. By 14 days, further dysregulation induces genes responding to cellular damage. The inability to relieve ER stress in the face of only partly abated production of secretory proteins leads to the induction of cellular destruction processes (autophagy, phagosomes, and lysosomes) and increased apoptosis.

The continued expression of *Ptf1a* is necessary for pancreatic acinar cell homeostasis. PTF1A engenders a fundamental state of instability by creating the burden of unfolded protein and RER redox stresses through its fundamental role as the principal driver of secretory enzyme gene transcription. PTF1A also counters such instability, however, by its direct action on homeostatic genes, such as UPR factors, ERAD components, and cell-specific folding enzymes (e.g., ERP27 and CABP2), to moderate and contend with high unfolded protein stress. The abrupt removal of PTF1A upsets this precarious steady state and leads to the disruption of acinar homeostasis in a cell-autonomous manner.

The adult PTF1A transcription factor network. Ten sequence-specific DNA-binding TFs form a pancreatic acinar transcriptional network with extensive cross-regulation (Fig. 7M). *Ptf1a*, *Rbpjl*, *Myc*, *Nr5a2*, and *Mist1* play key roles in pancreatic acinar development and the mature phenotype and form the network core. RBPJL is the partner of PTF1A in the PTF1-L complex. PTF1-L binds and controls the genes of this network. PTF1-L binds and activates the autoregulatory enhancer of *Ptf1a* (64) as well as the promoter of *Rbpjl* (25). Autoregulation of lineage-specific TFs is a common mechanism to lock cell fate decisions during development (65). In the adult pancreatic acinar cell, autoactivation by PTF1-L secures the continued transcription of *Ptf1a* and *Rbpjl* and thereby enforces the differentiated acinar phenotype.

The other members of the network core have key roles in acinar cell physiology. *Myc* is required for the replication of prenatal pancreatic (66, 67) and adult acinar cells (68). In our study, *Myc* mRNA was lost rapidly after *Ptf1a* inactivation, and the MYC-depleted cells were selectively unresponsive to the call for acinar cell regeneration. In many contexts MYC increases cell size (69), in part by raising protein synthesis through enhanced

expression of genes for ribosomal proteins and translation initiation factors (70). More than a hundred *Myc*-dependent genes are bound by and also dependent on PTF1A. Thus, PTF1A enhances acinar cell growth and sustains the high capacity of acinar protein synthesis by raising *Myc* expression and by collaborating with MYC at many MYC-dependent genes.

NR5A2 complements the acinar regulatory functions of PTF1A. During development, *Nr5a2* is required to complete the differentiation of acinar cells (40). Inactivation of *Nr5a2* in adult pancreas affected a limited set of genes principally associated with acinar secretion (58). Unlike the effects of *Ptf1a* inactivation, however, the loss of *Nr5a2* did not induce genes characteristic of duct, stomach, or any other identifiable cell type. Half of the *Nr5a2*-dependent genes (58) are also dependent on *Ptf1a* and are highly enriched for acinus-specific functions of digestive enzyme synthesis. Thus, NR5A2 has extensive acinar network responsibilities separately and in collaboration with PTF1A.

The scaling TF MIST1 enhances the secretory phenotype of many exocrine cells but does not specify a particular type of acinar cell (71). The pancreatic acinar epithelium that forms in *Mist1*-null mouse embryos is unstable, cellular architecture and gap junction communication are disrupted, and regulated exocytosis is affected adversely (72, 73). Several MIST1 target genes in pancreatic acinar cells, including *Rab3d*, *Ccp1*, *Serpini1*, *Reg1*, *Nupr1*, and *Rab26* (60), are bound by PTF1A at control regions and also are downregulated by inactivation of *Ptf1a*. Thus, PTF1A and MIST1 also collaborate at target genes. Indeed, we have recently shown that PTF1A and MIST1 collaborate extensively through reiterated feed-forward regulatory loops controlling acinar genes (102). The extensive regulatory relationships show that PTF1A collaborates with the other network core factors in feed-forward control strategies at large numbers of acinar genes.

PTF1-L binds and controls the genes of several additional highly expressed TFs, including *Gfi1*, *Tead2*, *Atf6*, *Nfatc1*, *Nfatc2*, *Spdef*, and *Ehf*. Roles for these downstream effectors of *Ptf1a* gene regulation in acinar differentiation, growth, transformation, or acinar-ductal metaplasia have been established for GFI1 (74), TEAD1/2 (75–77), and NFATC1/2 (78–81). SPDEF and EHF are key differentiation factors for other glandular cell types (82–86) and may play similar roles for the acinar pancreas. Together, the members of the network control a large fraction of the processes characteristic of the specialized physiology of the pancreatic acinar cell.

Pancreatic acinar cell identity. The adult pancreatic acinar cell, previously thought to be terminally and irreversibly differentiated, is now known to be surprisingly malleable (87–90). We showed that two critical aspects of regulation by *Ptf1a* define the acinar cell identity. First is the transcription of signature pancreatic acinar genes encoding the digestive enzymes and several equally restricted genes for secretory protein folding, intracellular transport, and zymogen granule packaging. The counterpoint is the suppression of genes characteristic of other cell types, especially pancreatic ductal cells and gastric gland cells.

The pancreatic and gastric gene-regulatory and developmental programs are related. Several pancreatic acinar secretory enzymes are produced in chief cells (91), and gastric markers are expressed at low levels in the normal pancreas (this study). The pancreas and stomach arise from nearby domains of the endoderm, and *Ptf1a* plays a key role in distinguishing the pancreas (12, 13, 25). Ectopic expression of *Ptf1a* in the anterior foregut endoderm at the onset

of organogenesis is sufficient to redirect development of the pre-stomach domain to the pancreas (92–94). Our results show a complementary effect: inactivation of *Ptf1a* in pancreatic acinar cells releases a suppressed gastric gene expression program encompassing all gastric cell lineages.

The gastric transcription factor MECOM (95) links the specific gastric genes and their induction in PTF1A-deficient pancreas. MECOM is a potential regulator of gastric gland-restricted genes (48), and the inherent low level of *Mecom* expression might be responsible for the small amount of *Chia*, *Pga5*, *Gif*, *Gkn3*, *Gcnt3*, and *Kcnj15* mRNAs in normal pancreas. The increase of *Mecom* expression soon after *Ptf1a* inactivation coincides with further induction of these six gastric mRNAs, and the continuing increase of *Mecom* mRNA correlates with the *de novo* activation of the set of pancreas-silent gastric genes.

A similar change of acinar cell identity extends to the loss of PTF1A and the appearance of gastric markers in early neoplastic lesions (PanINs) of pancreatic adenocarcinoma (96–98). MECOM has been proposed to play an early role in pancreatic cancer, in part by stimulating the accumulation of KRAS mRNA (48). An increase of active KRAS above a threshold through induction by MECOM might alter the state of acinar differentiation and increase susceptibility to malignant transformation (99). Changes in cellular identity are often a prelude to neoplasia (100, 101). Because PTF1A depletion greatly sensitizes acinar cells to KRAS-induced PanIN formation and pancreatic adenocarcinoma (23), we propose that the disruption of acinar cell identity by the loss of PTF1A establishes a more permissive state for transformation. In this scenario, the induction of gastric genes signals the disruption of acinar cell identity and the emergence of potentially oncogenic MECOM, linked properties of the permissive state.

ACKNOWLEDGMENTS

We thank Mark Borromeo, Rahul Kollipara, and Mei Jiang for assistance with bioinformatics, Jumin Xue for mouse husbandry and care, Jenna Jewell for help with phospho-RPS6 immunodetection, Steve Konieczny for MIST1 antibody, and Chaoying Liang, Quan-Zhen Li, and Ward Wakeland of the UT Southwestern Genomics and Microarray Core.

FUNDING INFORMATION

This work, including the efforts of Raymond J. MacDonald, was funded by HHS | NIH | National Institute of Diabetes and Digestive and Kidney Diseases (NIDDK) (DK61220). This work, including the efforts of Christopher V. E. Wright, was funded by HHS | NIH | National Institute of Diabetes and Digestive and Kidney Diseases (NIDDK) (DK89570). This work, including the efforts of Mark A. Magnuson, was funded by HHS | NIH | National Institute of Diabetes and Digestive and Kidney Diseases (NIDDK) (DK72473 and DK89523).

REFERENCES

- Slack JM. 2007. Metaplasia and transdifferentiation: from pure biology to the clinic. *Nat Rev Mol Cell Biol* 8:369–378. <http://dx.doi.org/10.1038/nrm2146>.
- Stanger BZ, Hebrok M. 2013. Control of cell identity in pancreas development and regeneration. *Gastroenterology* 144:1170–1179. <http://dx.doi.org/10.1053/j.gastro.2013.01.074>.
- Nashun B, Hill PWS, Hajkova P. 2015. Reprogramming of cell fate: epigenetic memory and the erasure of memories past. *EMBO J* 34:975–1142. <http://dx.doi.org/10.15252/embj.201591447>.
- Rajagopal J, Stanger BZ. 2016. Plasticity in the adult: how should the Waddington diagram be applied to regenerating tissues? *Dev Cell* 36:133–137. <http://dx.doi.org/10.1016/j.devcel.2015.12.021>.
- Heinz S, Romanoski CE, Benner C, Glass CK. 2015. The selection and

- function of cell type-specific enhancers. *Nat Rev Mol Cell Biol* 16:144–154. <http://dx.doi.org/10.1038/nrm3949>.
6. Whyte WA, Orlando DA, Hnisz D, Abraham BJ, Lin CY, Kagey MH, Rahl PB, Lee TI, Young RA. 2013. Master transcription factors and mediator establish super-enhancers at key cell identity genes. *Cell* 153:307–319. <http://dx.doi.org/10.1016/j.cell.2013.03.035>.
 7. Cahan P, Morris SA, Collins JJ, Daley GQ. 2014. Defining cellular identity through network biology. *Cell Cycle* 13:3313–3314. <http://dx.doi.org/10.4161/15384101.2014.972918>.
 8. Cahan P, Li H, Morris SA, Lummertz da Rocha E, Daley GQ, Collins JJ. 2014. CellNet: network biology applied to stem cell engineering. *Cell* 158:903–915. <http://dx.doi.org/10.1016/j.cell.2014.07.020>.
 9. Palade GE. 1992. Intracellular aspects of the process of protein secretion, p 177–206. *In* Lindsten J (ed), *Nobel lectures in physiology or medicine 1971-1980*. World Scientific Publishing, Singapore.
 10. Swift GH, Hammer RE, MacDonald RJ, Brinster RL. 1984. Tissue-specific expression of the rat pancreatic elastase I gene in transgenic mice. *Cell* 38:639–646. [http://dx.doi.org/10.1016/0092-8674\(84\)90258-7](http://dx.doi.org/10.1016/0092-8674(84)90258-7).
 11. Case M. 1978. Synthesis, intracellular transport and discharge of exportable proteins in the pancreatic acinar cell and other cells. *Biol Rev Camb Philos Soc* 53:211–354. <http://dx.doi.org/10.1111/j.1469-185X.1978.tb01437.x>.
 12. Kawaguchi Y, Cooper B, Gannon M, Ray M, MacDonald RJ, Wright CVE. 2002. The role of the transcriptional regulator PTF1a in converting intestinal to pancreatic progenitors. *Nat Genet* 32:128–134. <http://dx.doi.org/10.1038/ng959>.
 13. Krapp A, Knofler M, Ledermann B, Burki K, Berney C, Zoerkler N, Hagenbuchle O, Wellauer PK. 1998. The bHLH protein PTF1-p48 is essential for the formation of the exocrine and the correct spatial organization of the endocrine pancreas. *Genes Dev* 12:3752–3763. <http://dx.doi.org/10.1101/gad.12.23.3752>.
 14. Burlison JS, Long Q, Fujitani Y, Wright CV, Magnuson MA. 2008. Pdx-1 and Ptf1a concurrently determine fate specification of pancreatic multipotent progenitor cells. *Dev Biol* 316:74–86. <http://dx.doi.org/10.1016/j.ydbio.2008.01.011>.
 15. Dong PD, Provost E, Leach SD, Stainier DY. 2008. Graded levels of Ptf1a differentially regulate endocrine and exocrine fates in the developing pancreas. *Genes Dev* 22:1445–1450. <http://dx.doi.org/10.1101/gad.1663208>.
 16. Pan FC, Bankaitis ED, Boyer D, Xu X, Van de Castele M, Magnuson MA, Heimberg H, Wright CV. 2013. Spatiotemporal patterns of multipotentiality in Ptf1a-expressing cells during pancreas organogenesis and injury-induced facultative restoration. *Development* 140:751–764. <http://dx.doi.org/10.1242/dev.090159>.
 17. Thompson N, Gesina E, Scheinert P, Bucher P, Grapin-Botton A. 2012. RNA profiling and chromatin immunoprecipitation-sequencing reveal that PTF1a stabilizes pancreas progenitor identity via the control of MNX1/HLXB9 and a network of other transcription factors. *Mol Cell Biol* 32:1189–1199. <http://dx.doi.org/10.1128/MCB.06318-11>.
 18. Rose SD, Swift GH, Peyton MJ, Hammer RE, MacDonald RJ. 2001. The role of PTF1-P48 in pancreatic acinar gene expression. *J Biol Chem* 276:44018–44026. <http://dx.doi.org/10.1074/jbc.M106264200>.
 19. Masui T, Swift GH, Deering T, Shen C, Coats WS, Long Q, Elsasser HP, Magnuson MA, MacDonald RJ. 2010. Replacement of Rbpj with Rbpjl in the PTF1 complex controls the final maturation of pancreatic acinar cells. *Gastroenterology* 139:270–280. <http://dx.doi.org/10.1053/j.gastro.2010.04.003>.
 20. Rodolosse A, Campos ML, Rooman I, Lichtenstein M, Real FX. 2009. p/CAF modulates the activity of the transcription factor p48/Ptf1a involved in pancreatic acinar differentiation. *Biochem J* 418:463–473. <http://dx.doi.org/10.1042/BJ20080293>.
 21. Beres TM, Masui T, Swift GH, Shi L, Henke RM, MacDonald RJ. 2006. PTF1 is an organ-specific and Notch-independent basic helix-loop-helix complex containing the mammalian Suppressor of Hairless (RBP-J) or its paralogue, RBP-L. *Mol Cell Biol* 26:117–130. <http://dx.doi.org/10.1128/MCB.26.1.117-130.2006>.
 22. Molero X, Adell T, Skoudy A, Padilla MA, Gomez JA, Chaloux E, Malagelada JR, Real FX. 2007. Pancreas transcription factor 1alpha expression is regulated in pancreatitis. *Eur J Clin Invest* 37:791–801. <http://dx.doi.org/10.1111/j.1365-2362.2007.01856.x>.
 23. Krah NM, De La OJ, Swift GH, Hoang CQ, Willet SG, Chen Pan F, Cash GM, Bronner MP, Wright CV, MacDonald RJ, Murtaugh LC. 2015. The acinar differentiation determinant PTF1A inhibits initiation of pancreatic ductal adenocarcinoma. *eLife* 4:e07125. <http://dx.doi.org/10.7554/eLife.07125>.
 24. Obata J, Yano M, Mimura H, Goto T, Nakayama R, Mibu Y, Oka C, Kawaichi M. 2001. p48 subunit of mouse PTF1 binds to RBP-Jk/CBF1, the intracellular mediator of Notch signalling, and is expressed in the neural tube of early stage embryos. *Genes Cells* 6:345–360. <http://dx.doi.org/10.1046/j.1365-2443.2001.00422.x>.
 25. Masui T, Long Q, Beres TM, Magnuson MA, MacDonald RJ. 2007. Early pancreatic development requires the vertebrate Suppressor of Hairless (RBPJ) in the PTF1 bHLH complex. *Genes Dev* 21:2629–2643. <http://dx.doi.org/10.1101/gad.1575207>.
 26. Meredith DM, Borromeo MD, Deering TG, Casey B, Savage TK, Mayer PR, Hoang C, Tung KC, Kumar M, Shen C, Swift GH, MacDonald RJ, Johnson JE. 2013. Program specificity for Ptf1a in pancreas versus neural tube development correlates with distinct collaborating cofactors and chromatin accessibility. *Mol Cell Biol* 33:3166–3179. <http://dx.doi.org/10.1128/MCB.00364-13>.
 27. Kopan R, Ilagan MX. 2009. The canonical Notch signaling pathway: unfolding the activation mechanism. *Cell* 137:216–233. <http://dx.doi.org/10.1016/j.cell.2009.03.045>.
 28. Johnson JE, MacDonald RJ. 2011. Notch-independent functions of CSL. *Curr Top Dev Biol* 97:55–74. <http://dx.doi.org/10.1016/B978-0-12-385975-4.00009-7>.
 29. Minoguchi S, Taniguchi Y, Kato H, Okazaki T, Strobl LJ, Zimmer-Strobl U, Bornkamm GW, Honjo T. 1997. RBP-L, a transcription factor related to RBP-Jk. *Mol Cell Biol* 17:2679–2687. <http://dx.doi.org/10.1128/MCB.17.5.2679>.
 30. Hayashi S, McMahon AP. 2002. Efficient recombination in diverse tissues by a tamoxifen-inducible form of Cre: a tool for temporally regulated gene activation/inactivation in the mouse. *Dev Biol* 244:305–318. <http://dx.doi.org/10.1006/dbio.2002.0597>.
 31. Chirgwin JM, Przybyla AE, MacDonald RJ, Rutter WJ. 1979. Isolation of biologically active ribonucleic acid from sources enriched in ribonuclease. *Biochemistry* 24:5294–5299.
 32. MacDonald RJ, Swift GH, Przybyla AE, Chirgwin JM. 1987. Isolation of RNA using guanidinium salts. *Methods Enzymol* 152:219–227. [http://dx.doi.org/10.1016/0076-6879\(87\)52023-7](http://dx.doi.org/10.1016/0076-6879(87)52023-7).
 33. Harding JD, MacDonald RJ, Przybyla AE, Chirgwin JM, Pictet RL, Rutter WJ. 1977. Changes in the frequency of specific transcripts during development of the pancreas. *J Biol Chem* 252:7391–7397.
 34. Githens S. 1988. The pancreatic duct cell: proliferative capabilities, specific characteristics, metaplasia, isolation and culture. *J Pediatr Gastroenterol Nutr* 7:486–506. <http://dx.doi.org/10.1097/00005176-198807000-00004>.
 35. McCarthy DJ, Chen Y, Smyth GK. 2012. Differential expression analysis of multifactor RNA-Seq experiments with respect to biological variation. *Nucleic Acids Res* 40:4288–4297. <http://dx.doi.org/10.1093/nar/gks042>.
 36. Anders S, Huber W. 2010. Differential expression analysis for sequence count data. *Genome Biol* 11:R106. <http://dx.doi.org/10.1186/gb-2010-11-10-r106>.
 37. Robinson MD, McCarthy DJ, Smyth GK. 2010. edgeR: a Bioconductor package for differential expression analysis of digital gene expression data. *Bioinformatics* 26:139–140. <http://dx.doi.org/10.1093/bioinformatics/btp616>.
 38. R Core Team. 2015. R: a language and environment for statistical computing. R Foundation for Statistical Computing, Vienna, Austria. <http://www.R-project.org>.
 39. Samali A, Fitzgerald U, Deegan S, Gupta S. 2010. Methods for monitoring endoplasmic reticulum stress and the unfolded protein response. *Int J Cell Biol* 2010:830307. <http://dx.doi.org/10.1155/2010/830307>.
 40. Hale MA, Swift GH, Hoang CQ, Deering TG, Masui T, Lee YK, Xue J, MacDonald RJ. 2014. The nuclear hormone receptor family member NR5A2 controls aspects of multipotent progenitor cell-formation and acinar differentiation during pancreatic organogenesis. *Development* 141:1–11. <http://dx.doi.org/10.1242/dev.109405>.
 41. Madisen L, Zwingman TA, Sunkin SM, Oh SW, Zariwala HA, Gu H, Ng LL, Palmeter RD, Hawrylycz MJ, Jones AR, Lein ES, Zeng H. 2010. A robust and high-throughput Cre reporting and characterization system for the whole mouse brain. *Nat Neurosci* 13:133–140. <http://dx.doi.org/10.1038/nn.2467>.
 42. McLean CY, Bristor D, Hiller M, Clarke SL, Schaar BT, Lowe CB, Wenger AM, Bejerano G. 2010. GREAT improves functional interpretation of genomic regions. *Nat Methods* 7:837–841. <http://dx.doi.org/10.1038/nmeth1445>.

- tation of cis-regulatory regions. *Nat Biotechnol* 28:495–501. <http://dx.doi.org/10.1038/nbt.1630>.
43. Crozier SJ, D'Alecy LG, Ernst SA, Ginsburg LE, Williams JA. 2009. Molecular mechanisms of pancreatic dysfunction induced by protein malnutrition. *Gastroenterology* 137:1093–1101. <http://dx.doi.org/10.1053/j.gastro.2009.04.058>.
 44. Ohta E, Itoh T, Nemoto T, Kumagai J, Ko SB, Ishibashi K, Ohno M, Uchida K, Ohta A, Sohara E, Uchida S, Sasaki S, Rai T. 2009. Pancreas-specific aquaporin 12 null mice showed increased susceptibility to caerulein-induced acute pancreatitis. *Am J Physiol Cell Physiol* 297:C1368–C1378. <http://dx.doi.org/10.1152/ajpcell.00117.2009>.
 45. Kimura MS, Mutoh H, Sugano K. 2011. SOX9 is expressed in normal stomach, intestinal metaplasia, and gastric carcinoma in humans. *J Gastroenterol* 46:1292–1299. <http://dx.doi.org/10.1007/s00535-011-0443-5>.
 46. McCracken KW, Cata EM, Crawford CM, Sinagoga KL, Schumacher M, Rockich BE, Tsai YH, Mayhew CN, Spence JR, Zavros Y, Wells JM. 2014. Modelling human development and disease in pluripotent stem-cell-derived gastric organoids. *Nature* 516:400–404. <http://dx.doi.org/10.1038/nature13863>.
 47. Kim TH, Shivdasani RA. 2011. Notch signaling in stomach epithelial stem cell homeostasis. *J Exp Med* 208:677–688. <http://dx.doi.org/10.1084/jem.20101737>.
 48. Tanaka M, Suzuki HI, Shibahara J, Kunita A, Isagawa T, Yoshimi A, Kurokawa M, Miyazono K, Aburatani H, Ishikawa S, Fukayama M. 2014. EVI1 oncogene promotes KRAS pathway through suppression of microRNA-96 in pancreatic carcinogenesis. *Oncogene* 33:2454–2463. <http://dx.doi.org/10.1038/ncr.2013.204>.
 49. Barreto SG, Carati CJ, Toouli J, Saccone GT. 2010. The islet-acinar axis of the pancreas: more than just insulin. *Am J Physiol Gastrointest Liver Physiol* 299:G10–G22. <http://dx.doi.org/10.1152/ajpgi.00077.2010>.
 50. Williams JA, Sans MD, Tashiro M, Schafer C, Bragado MJ, Dabrowski A. 2002. Cholecystokinin activates a variety of intracellular signal transduction mechanisms in rodent pancreatic acinar cells. *Pharmacol Toxicol* 91:297–303. <http://dx.doi.org/10.1034/j.1600-0773.2002.910606.x>.
 51. Williams JA. 2008. Receptor-mediated signal transduction pathways and the regulation of pancreatic acinar cell function. *Curr Opin Gastroenterol* 24:573–579. <http://dx.doi.org/10.1097/MOG.0b013e32830b110c>.
 52. Siveke JT, Lubeseder-Martellato C, Lee M, Mazur PK, Nakhai H, Radtke F, Schmid RM. 2008. Notch signaling is required for exocrine regeneration after acute pancreatitis. *Gastroenterology* 134:544–555. <http://dx.doi.org/10.1053/j.gastro.2007.11.003>.
 53. Keefe MD, Wang H, De La OJ, Khan A, Firpo MA, Murtaugh LC. 2012. Beta-catenin is selectively required for the expansion and regeneration of mature pancreatic acinar cells in mice. *Dis Model Mech* 5:503–514. <http://dx.doi.org/10.1242/dmm.007799>.
 54. Watsons RJ, Eyden BP, Howell A, Sellwood RA. 1988. Ultrastructural observations on the basal lamina in the normal human breast. *J Anat* 156:1–10.
 55. Vaccaro MI. 2012. Zymophagy: selective autophagy of secretory granules. *Int J Cell Biol* 2012:396705. <http://dx.doi.org/10.1155/2012/396705>.
 56. Gorelick FS, Adler G, Kern HF. 1993. Cerulein-induced pancreatitis, p 501–526. *In* Go VLE, DiMugno EP, Gardner JD, Leberthal E, Reber HA, Scheele GA (ed), *The pancreas: biology, pathobiology and disease*, 2nd ed. Raven Press, New York, NY.
 57. Masamune A, Shimosegawa T. 2013. Pancreatic stellate cells—multifunctional cells in the pancreas. *Pancreatol* 13:102–105. <http://dx.doi.org/10.1016/j.pan.2012.12.058>.
 58. Holmstrom SR, Deering T, Swift GH, Poelwijk FJ, Mangelsdorf DJ, Kliewer SA, MacDonald RJ. 2011. LXR-1 and PTF1-L coregulate an exocrine pancreas-specific transcriptional network for digestive function. *Genes Dev* 25:1674–1679. <http://dx.doi.org/10.1101/gad.16860911>.
 59. Chaillou T, Kirby TJ, McCarthy JJ. 2014. Ribosome biogenesis: emerging evidence for a central role in the regulation of skeletal muscle mass. *J Cell Physiol* 229:1584–1594. <http://dx.doi.org/10.1002/jcp.24604>.
 60. Drenzo D, Hess DA, Damsz B, Hallett JE, Marshall B, Goswami C, Liu Y, Deering T, MacDonald RJ, Konieczny SF. 2012. Induced Mist1 expression promotes remodeling of mouse pancreatic acinar cells. *Gastroenterology* 143:469–480. <http://dx.doi.org/10.1053/j.gastro.2012.04.011>.
 61. Jin RU, Mills JC. 2014. RAB26 coordinates lysosome traffic and mitochondrial localization. *J Cell Sci* 127:1018–1032. <http://dx.doi.org/10.1242/jcs.138776>.
 62. Logsdon CD, Ji B. 2013. The role of protein synthesis and digestive enzymes in acinar cell injury. *Nat Rev Gastroenterol Hepatol* 10:362–370. <http://dx.doi.org/10.1038/nrgastro.2013.36>.
 63. MacDonald RJ, Swift GH, Real FX. 2010. Transcriptional control of exocrine pancreas development and homeostasis, p 1–40. *In* Kaestner KH (ed), *Development, differentiation and disease of the para-alimentary tract*, vol 97. Academic Press, Burlington, VT.
 64. Masui M, Swift GH, Hale MA, Meredith D, Johnson JE, MacDonald RJ. 2008. Transcriptional autoregulation controls pancreatic Ptf1a expression during development and adulthood. *Mol Cell Biol* 28:5458–5468. <http://dx.doi.org/10.1128/MCB.00549-08>.
 65. Holmberg J, Perlmann T. 2012. Maintaining differentiated cellular identity. *Nat Rev Genet* 13:429–439. <http://dx.doi.org/10.1038/nrg3209>.
 66. Nakhai H, Siveke JT, Mendoza-Torres L, Schmid RM. 2008. Conditional inactivation of Myc impairs development of the exocrine pancreas. *Development* 135:3191–3196. <http://dx.doi.org/10.1242/dev.017137>.
 67. Bonal C, Thorel F, Ait-Lounis A, Reith W, Trumpp A, Herrera PL. 2009. Pancreatic inactivation of c-Myc decreases acinar mass and trans-differentiates acinar cells into adipocytes in mice. *Gastroenterology* 136:309–319. <http://dx.doi.org/10.1053/j.gastro.2008.10.015>.
 68. Cendrowski J, Lobo VJ, Sendler M, Salas A, Kuhn JP, Molero X, Fukunaga R, Mayerle J, Lerch MM, Real FX. 2015. Mnk1 is a novel acinar cell-specific kinase required for exocrine pancreatic secretion and response to pancreatitis in mice. *Gut* 64:937–947. <http://dx.doi.org/10.1136/gutjnl-2013-306068>.
 69. Eilers M, Eisenman RN. 2008. Myc's broad reach. *Genes Dev* 22:2755–2766. <http://dx.doi.org/10.1101/gad.1712408>.
 70. van Riggelen J, Yetil A, Felsher DW. 2010. MYC as a regulator of ribosome biogenesis and protein synthesis. *Nat Rev Cancer* 10:301–309. <http://dx.doi.org/10.1038/nrc2819>.
 71. Mills JC, Taghert PH. 2012. Scaling factors: transcription factors regulating subcellular domains. *Bioessays* 34:10–16. <http://dx.doi.org/10.1002/bies.201100089>.
 72. Luo X, Shin DM, Wang X, Konieczny SF, Muallem S. 2005. Aberrant localization of intracellular organelles, Ca²⁺ signaling, and exocytosis in Mist1 null mice. *J Biol Chem* 280:12668–12675. <http://dx.doi.org/10.1074/jbc.M411973200>.
 73. Shi G, Zhu L, Sun Y, Bettencourt R, Damsz B, Hruban RH, Konieczny SF. 2009. Loss of the acinar-restricted transcription factor Mist1 accelerates Kras-induced pancreatic intraepithelial neoplasia. *Gastroenterology* 136:1368–1378. <http://dx.doi.org/10.1053/j.gastro.2008.12.066>.
 74. Sarkar SA, Lee CE, Tipney H, Karimpour-Fard A, Dinella JD, Juhl K, Walters JA, Hutton JC, Hunter LE. 2012. Synergizing genomic analysis with biological knowledge to identify and validate novel genes in pancreatic development. *Pancreas* 41:962–969. <http://dx.doi.org/10.1097/MPA.0b013e31823d0160>.
 75. Cebola I, Rodriguez-Segui SA, Cho CH, Bessa J, Rovira M, Luengo M, Chhatrivala M, Berry A, Ponsa-Cobas J, Maestro MA, Jennings RE, Pasquali L, Moran I, Castro N, Hanley NA, Gomez-Skarmeta JL, Vallier L, Ferrer J. 2015. TEAD and YAP regulate the enhancer network of human embryonic pancreatic progenitors. *Nat Cell Biol* 17:615–626. <http://dx.doi.org/10.1038/ncb3160>.
 76. Gao T, Zhou D, Yang C, Singh T, Penzo-Mendez A, Maddipati R, Tzatsos A, Bardeesy N, Avruch J, Stanger BZ. 2013. Hippo signaling regulates differentiation and maintenance in the exocrine pancreas. *Gastroenterology* 144:1543–1553. <http://dx.doi.org/10.1053/j.gastro.2013.02.037>.
 77. Moroishi T, Hansen CG, Guan KL. 2015. The emerging roles of YAP and TAZ in cancer. *Nat Rev Cancer* 15:73–79. <http://dx.doi.org/10.1038/nrc3876>.
 78. Chen NM, Singh G, Koenig A, Liou GY, Storz P, Zhang JS, Regul L, Nagarajan S, Kuhnemuth B, Johnsen SA, Hebrak M, Siveke J, Billadeau DD, Ellenrieder V, Hessmann E. 2015. NFATc1 links EGFR signaling to induction of Sox9 transcription and acinar-ductal transdifferentiation in the pancreas. *Gastroenterology* 148:1024–1034. <http://dx.doi.org/10.1053/j.gastro.2015.01.033>.
 79. Gurda GT, Guo L, Lee SH, Molkenint JD, Williams JA. 2008. Cholecystokinin activates pancreatic calcineurin-NFAT signaling in vitro and in vivo. *Mol Biol Cell* 19:198–206. <http://dx.doi.org/10.1091/mbc.E07-05-0430>.
 80. Buchholz M, Schatz A, Wagner M, Michl P, Linhart T, Adler G, Gress TM, Ellenrieder V. 2006. Overexpression of c-myc in pancreatic cancer caused by ectopic activation of NFATc1 and the Ca²⁺/calcineurin sig-

- naling pathway. *EMBO J* 25:3714–3724. <http://dx.doi.org/10.1038/sj.emboj.7601246>.
81. Gurda GT, Crozier SJ, Ji B, Ernst SA, Logsdon CD, Rothermel BA, Williams JA. 2010. Regulator of calcineurin 1 controls growth plasticity of adult pancreas. *Gastroenterology* 139:609–619. <http://dx.doi.org/10.1053/j.gastro.2010.04.050>.
 82. Chen G, Korfhagen TR, Xu Y, Kitzmiller J, Wert SE, Maeda Y, Gregorieff A, Clevers H, Whitsett JA. 2009. SPDEF is required for mouse pulmonary goblet cell differentiation and regulates a network of genes associated with mucus production. *J Clin Invest* 119:2914–2924. <http://dx.doi.org/10.1172/JCI39731>.
 83. Gregorieff A, Stange DE, Kujala P, Begthel H, van den Born M, Korving J, Peters PJ, Clevers H. 2009. The ets-domain transcription factor Spdef promotes maturation of goblet and Paneth cells in the intestinal epithelium. *Gastroenterology* 137:1333–1345. <http://dx.doi.org/10.1053/j.gastro.2009.06.044>.
 84. Buchwalter G, Hickey MM, Cromer A, Selfors LM, Gunawardane RN, Frishman J, Jeselsohn R, Lim E, Chi D, Fu X, Schiff R, Brown M, Brugge JS. 2013. PDEF promotes luminal differentiation and acts as a survival factor for ER-positive breast cancer cells. *Cancer Cell* 23:753–767. <http://dx.doi.org/10.1016/j.ccr.2013.04.026>.
 85. Albino D, Longoni N, Curti L, Mello-Grand M, Pinton S, Civenni G, Thalmann G, D'Ambrosio G, Sarti M, Sessa F, Chiorino G, Catapano CV, Carbone GM. 2012. ESE3/EHF controls epithelial cell differentiation and its loss leads to prostate tumors with mesenchymal and stem-like features. *Cancer Res* 72:2889–2900. <http://dx.doi.org/10.1158/0008-5472.CAN-12-0212>.
 86. Stephens DN, Klein RH, Salmans ML, Gordon W, Ho H, Andersen B. 2013. The Ets transcription factor EHF as a regulator of cornea epithelial cell identity. *J Biol Chem* 288:34304–34324. <http://dx.doi.org/10.1074/jbc.M113.504399>.
 87. Ziv O, Glaser B, Dor Y. 2013. The plastic pancreas. *Dev Cell* 26:3–7. <http://dx.doi.org/10.1016/j.devcel.2013.06.013>.
 88. Valdez IA, Teo AK, Kulkarni RN. 2015. Cellular stress drives pancreatic plasticity. *Sci Transl Med* 7:273ps2.
 89. Merrell AJ, Stanger BZ. 2016. Adult cell plasticity in vivo: de-differentiation and transdifferentiation are back in style. *Nat Rev Mol Cell Biol* 17:413–425. <http://dx.doi.org/10.1038/nrm.2016.24>.
 90. Li W, Nakanishi M, Zumsteg A, Shear M, Wright C, Melton DA, Zhou Q. 2014. In vivo reprogramming of pancreatic acinar cells to three islet endocrine subtypes. *eLife* 3:e01846. <http://dx.doi.org/10.7554/eLife.01846.001>.
 91. Davis BP, Messing A, Hammer RE, MacDonald RJ. 1992. Selective expression of trypsin fusion genes in acinar cells of pancreas and stomach of transgenic mice. *J Biol Chem* 267:26070–26077.
 92. Willet SG, Hale MA, Grapin-Botton A, Magnuson MA, MacDonald RJ, Wright CV. 2014. Dominant and context-specific control of endodermal organ allocation by Ptf1a. *Development* 141:4385–4394. <http://dx.doi.org/10.1242/dev.114165>.
 93. Jarikji ZH, Vanamala S, Beck CW, Wright CV, Leach SD, Horb ME. 2007. Differential ability of Ptf1a and Ptf1a-VP16 to convert stomach, duodenum and liver to pancreas. *Dev Biol* 304:786–799. <http://dx.doi.org/10.1016/j.ydbio.2007.01.027>.
 94. Afelik S, Chen Y, Pieler T. 2006. Combined ectopic expression of Pdx1 and Ptf1a/p48 results in the stable conversion of posterior endoderm into endocrine and exocrine pancreatic tissue. *Genes Dev* 20:1441–1446. <http://dx.doi.org/10.1101/gad.378706>.
 95. Yatsula B, Lin S, Read AJ, Poholek A, Yates K, Yue D, Hui P, Perkins AS. 2005. Identification of binding sites of EVI1 in mammalian cells. *J Biol Chem* 280:30712–30722. <http://dx.doi.org/10.1074/jbc.M504293200>.
 96. Prasad NB, Biankin AV, Fukushima N, Maitra A, Dhara S, Elkhouloun AG, Hruban RH, Goggins M, Leach SD. 2005. Gene expression profiles in pancreatic intraepithelial neoplasia reflect the effects of Hedgehog signaling on pancreatic ductal epithelial cells. *Cancer Res* 65:1619–1626. <http://dx.doi.org/10.1158/0008-5472.CAN-04-1413>.
 97. Kim GE, Bae HI, Park HU, Kuan SF, Crawley SC, Ho JJ, Kim YS. 2002. Aberrant expression of MUC5AC and MUC6 gastric mucins and sialyl Tn antigen in intraepithelial neoplasms of the pancreas. *Gastroenterology* 123:1052–1060. <http://dx.doi.org/10.1053/gast.2002.36018>.
 98. Tanaka M, Shibahara J, Fukushima N, Shinozaki A, Umeda M, Ishikawa S, Kokudo N, Fukayama M. 2011. Claudin-18 is an early-stage marker of pancreatic carcinogenesis. *J Histochem Cytochem* 59:942–952. <http://dx.doi.org/10.1369/0022155411420569>.
 99. Logsdon CD, Ji B. 2009. Ras activity in acinar cells links chronic pancreatitis and pancreatic cancer. *Clin Gastroenterol Hepatol* 7:S40–S43. <http://dx.doi.org/10.1016/j.cgh.2009.07.040>.
 100. Puri S, Foliass AE, Hebrok M. 2015. Plasticity and dedifferentiation within the pancreas: development, homeostasis, and disease. *Cell Stem Cell* 16:18–31. <http://dx.doi.org/10.1016/j.stem.2014.11.001>.
 101. Roy N, Hebrok M. 2015. Regulation of cellular identity in cancer. *Dev Cell* 35:674–684. <http://dx.doi.org/10.1016/j.devcel.2015.12.001>.
 102. Jiang M, Azevedo-Pouly AC, Deering TG, Hoang CQ, DiRenzo DG, Hess DA, Konieczny ST, Swift GH, MacDonald RJ. 2016. MIST1 and PTF1 collaborate in feed-forward regulatory loops that maintain the pancreatic acinar phenotype in adult mice. *Mol Cell Biol* 36:2945–2955. <http://dx.doi.org/10.1128/MCB.00370-16>.